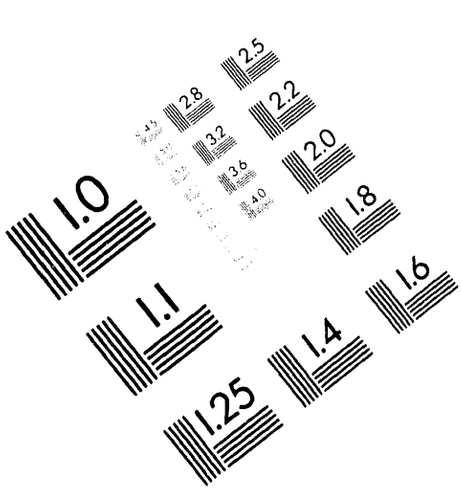

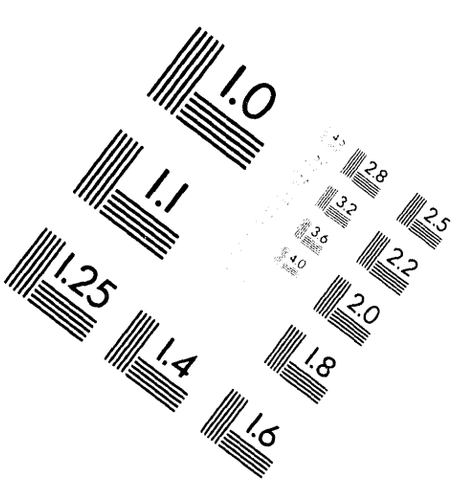

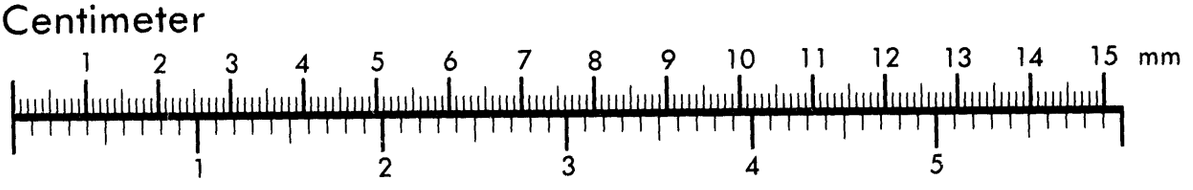

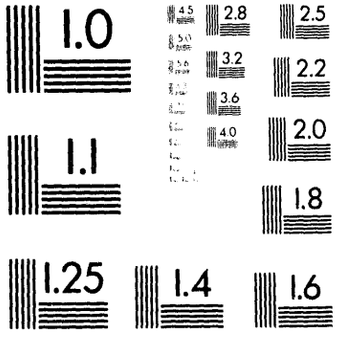

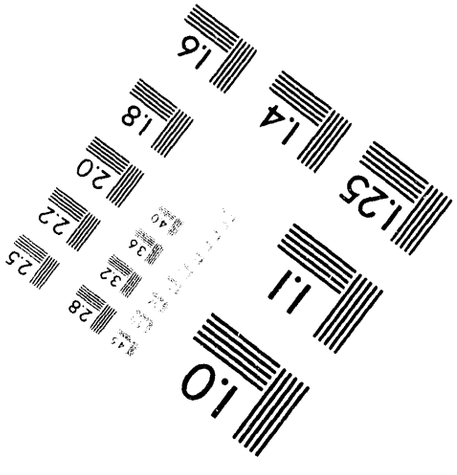

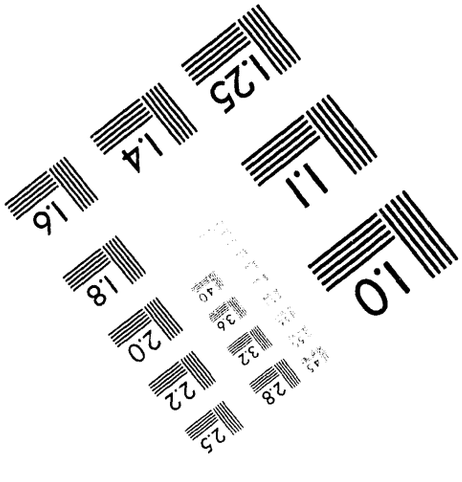

Association for Information and Image Management
1100 Wayne Avenue, Suite 1100
Silver Spring, Maryland 20910
301/587-8202

1 of 1

2/5-20-94950

UCRL-ID-116122

Preliminary Report on the Isotope Hydrology Investigations at the Nevada Test Site: Hydrologic Resources Management Program

FY 1992-1993

M. L. Davisson
J. M. Kenneally
D. K. Smith
G. B. Hudson
G. J. Nimz
J. H. Rego

Nuclear Chemistry Division
Lawrence Livermore National Laboratory

January 1994

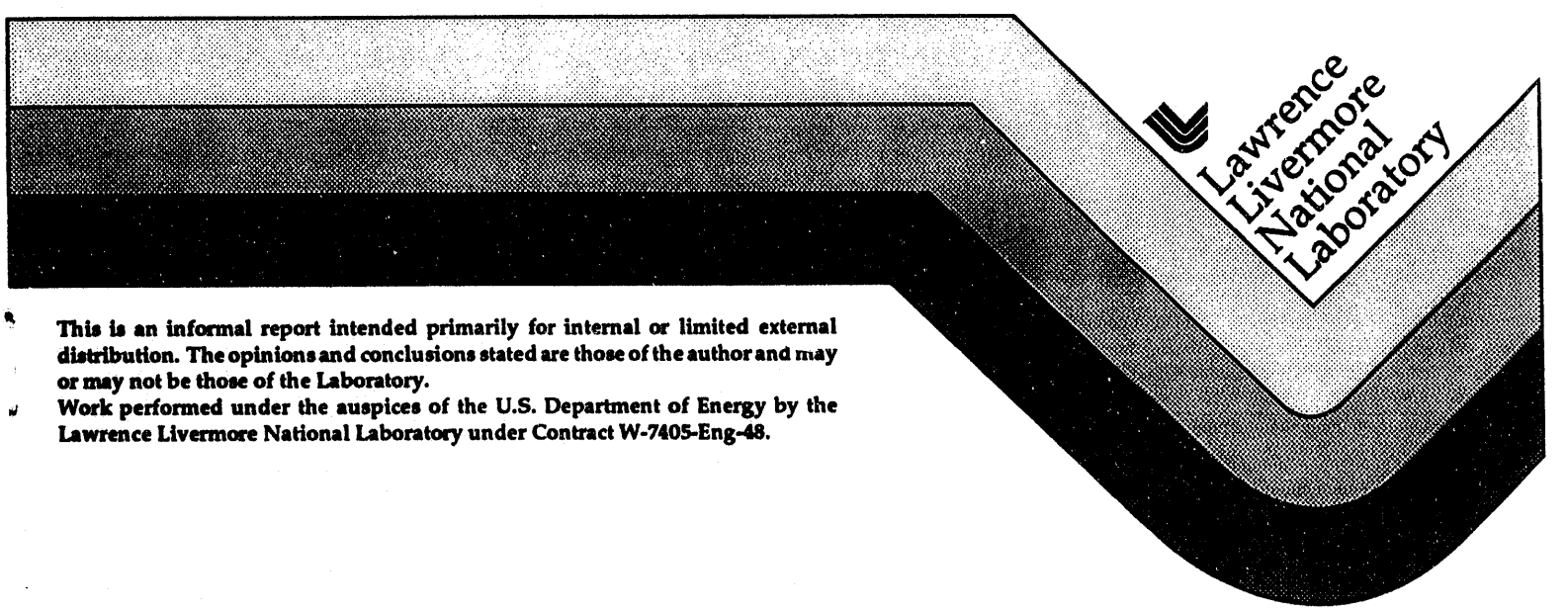

DISCLAIMER

PRELIMINARY REPORT ON THE ISOTOPE HYDROLOGY INVESTIGATIONS AT THE NEVADA TEST SITE: HYDROLOGIC RESOURCES MANAGEMENT PROGRAM FY 1992-1993

by

M.L. Davisson

J. M. Kenneally

D.K. Smith

G.B. Hudson

G.J. Nimz

J.H. Rego

Nuclear Chemistry Division

Lawrence Livermore National Laboratory

ABSTRACT

A comprehensive isotope data base of the NTS groundwaters collected during FY 92-93 is presented with preliminary interpretations. Multiple samples were collected from over 30 sites on pumped wells and open-holes by wireline bailing. Field water level measurements indicate essentially a bimodal distribution separated by water levels at higher elevations (e.g. Pahute Mesa) from water levels of lower elevations (e.g. Yucca and Frenchman Flats). Down hole temperature measurements have confirmed anomalous temperature gradients in the eastern Yucca Flat area and on Pahute Mesa, where horizontal temperature gradients up to 0.33°F/100ft are found.

Consistent with previous reports by others, the major ion geochemistry of the NTS groundwater are dominated by Na-K-HCO_3 and Ca-Mg-HCO_3 water types, where the Na-rich water appears to be related to dissolution in the volcanic tuffs and the Ca-rich water to the Paleozoic carbonates. Increases in dissolved Si also seems to be indicative of groundwater that resides in the volcanic tuffs. Processes controlling the Na/Ca ratios are complex and may include ion exchange reactions with clays, evaporative concentration in the vadose zone, and lithological heterogeneities in addition to simple differential dissolution between the volcanic tuffs and the Paleozoic carbonates.

Apparent ^{14}C ages range between 4000 and 38,000 years for groundwaters at the NTS. The uncertainty is large for exact age determinations at this time. The ^{14}C abundance decreases with increased dissolved HCO_3, and ^{13}C suggests dissolution of the "dead" Paleozoic carbonates significantly influence the ages, but more work is needed to investigate the influence of vadose zone carbonate.

The $^{36}Cl/Cl$ ratios measured in the NTS groundwaters do not indicate the presence of very old groundwater. Most of the decrease in the ^{36}Cl concentrations may be attributed to addition of a "dead" chloride from dissolution of the Paleozoic carbonates and the volcanic tuffs.

The $^{87}Sr/^{86}Sr$ measurements of the dissolved Sr in the NTS groundwaters indicate that a less radiogenic signature is characteristic of higher Si concentrations related to the volcanic tuffs, where more radiogenic values are associated with higher bicarbonate concentrations or the Paleozoic carbonates. Lithological heterogeneities and secondary mineralization may be the major controls on the $^{87}Sr/^{86}Sr$ ratios of the NTS groundwaters and further investigations, particularly of the solid phase, are needed.

Contaminant characterization of selected fission related radionuclides is in progress for all wells in addition to drill back holes in explosion cavities. Low-level tritium analyses indicate that all wells, with the exception of the drill back wells, fall well below the drinking water standards. Many of the wells are tritium "dead" indicating old groundwater (>100 years), where some wells may suggests some anthropogenic levels of tritium of very low levels, but analytical questions exist and re-analysis is needed. Well UE-5n shows abnormal tritium level of approximately 9900 pCi/L or half the drinking water standard. The tritium source probably originates from infiltration of Cambric ditch tritiated water, and is consistent with fluid rate calculations. Field measurements of tritium levels in the drill back holes vary up to 5 orders of magnitude, with the highest occurring in well U-4u at approximately 10^7 pCi/L.

The $^{234}U/^{238}U$ values measured in the NTS groundwaters during FY 92-93 are not included in this report and are undergoing data reduction. A review of previous work on $^{234}U/^{238}U$ at the NTS is presented.

Measured noble gas abundances in the water supply wells are anticipated in the near future. The data should yield information regarding the recharge temperatures and elevation of the groundwater. In addition, ^{4}He concentrations can be calibrated against the ^{14}C abundances to derive an independent groundwater age, and an example is presented.

TABLE OF CONTENTS page

INTRODUCTION

The Hydrologic Resources Management Program (HRMP) is administered by the Department of Energy Nevada Operations Office and has as its focus the groundwater of the Nevada Test Site (NTS) and surrounding regions of Nevada and eastern California. Two of the central responsibilities of the program are groundwater protection and groundwater monitoring at the NTS. In order to fulfill these responsibilities, generating adequate information to understand the NTS hydrologic system is required. Such information makes it possible to develop measures needed to protect the groundwater from contamination, due to the various activities on the NTS, and to develop strategies for a its satisfactory monitoring. Therefore it becomes one of the responsibilities of the HRMP to use its resources to aid in what is now a decades-long effort by many agencies to better characterize the hydrologic system underlying the NTS. The Nuclear Chemistry Division of the Lawrence Livermore National Laboratory has facilities and capabilities for isotopic and hydrochemical characterization of water that are unique within the HRMP. Part of the LLNL-HRMP effort has therefore been directed in the area of isotope hydrology at the NTS. This document reports the preliminary finding of this work, that was conducted during the 1992 and 1993 fiscal years. The large amount of isotopic and hydrochemical data produced is initially directed at data interpretation in this report, and will ultimately be synthesized with existing the physical hydrologic data. Therefore, this document is only preliminary to finalized reports that will be able to provide a broader understanding of the significance of the data and its relationship to groundwater flow at the NTS.

The ultimate goal of this work is to construct a hydro-isotopic framework that will characterize the groundwater at the NTS in terms of its recharge and discharge, flow directions and rates, and the origin of its dissolved constituents. The analytical techniques employ a suite of isotopic measurements of major and minor elements dissolved in or combined with the groundwater mass. Included in this suite are stable

isotopes ^{18}O, deuterium, ^{13}C, ^{3}He, ^{4}He, cosmogenic nuclides ^{14}C, and ^{36}Cl, radiogenic nuclides $^{87}Sr/^{86}Sr$, $^{234}U/^{238}U$, and noble gas abundances. Many techniques using these isotopes have been developed in other groundwater basins (see Fritz and Fontes, 1986 for summary), but only in rare cases have such a diverse group of isotopes been applied collectively to acquire detailed knowledge of groundwater (see Nordstrom et al., 1989 and accompanied articles; Fröhlich et al, 1991; Pearson et al., 199?).

HYDROGEOLOGIC BACKGROUND

The southwestern Nevada groundwater province consists predominantly of miogeoclinal Precambrian to Paleozoic sedimentary rocks of the western Cordilleran that incorporate evidence of a repeated history of tectonic shortening, followed by late-Cenozoic Basin-and-Range extension. The stratigraphic thickness of the Precambrian to Paleozoic section is in excess of 12 kilometers. Potable goundwater in these rocks can be found to depths in excess of 3000 meters from the earth's surface (Winograd and Thordarson, 1975; Mifflin and Hess, 1979). The sedimentary rocks are composed of approximately equal proportions of marine siliciclastics and carbonates. Overlying the sedimentary section are >4000 meters of late-Cenozoic volcanic rocks erupted concurrently with the Basin-and-Range tectonic extension. They consist predominantly of rhyolitic lavas and ash-flow tuffs, with minor basalt flows and sedimentary deposits (Winograd and Thordarson, 1975). The closed basins formed by the extension, for example Yucca Flat and Frenchman Flat on the NTS, that contain up to 600 meters of poorly-sorted alluvium.

The most extensive hydrogeologic framework constructed for the NTS was by Winograd and Thordarson (1975) where, based on detailed geologic investigations, pump test data, and major ion chemistry, they inferred a regional model for groundwater flow extending from the Pahranagat Valley (to the northeast) to Death Valley (to the southwest). Discharge occurs in the Death Valley region, and in Oasis Valley and Ash

Meadows in the Amargosa desert. The regional flow is considered dominant in the Paleozoic carbonate rocks. Winograd and Thordarson (1975) characterized the groundwater of Yucca and Frenchman Flats as being semiperched, predominantly saturating the tuff aquitard, and moving downward into the underlying Paleozoic carbonates. In all, Winograd and Thordarson recognized 10 separate hydrogeologic units (flow subsystems) at the NTS.

Blankennagel and Weir (1973) characterized the hydrogeology of the Pahute Mesa region where they noted that the groundwater flow appears to be independent of the complex volcanic stratigraphy, but locally controlled by faults and fractures within the rock. They concluded that groundwater flow was from the Mesa southwestward into the Amargosa Desert in aquifer material with transmissivities ranging from 1400 to 140000 gallons per day per foot. The relationship between the Pahute Mesa volcanic aquifers and the regional carbonate aquifers is poorly understood. Also unclear, is the nature of the groundwater system in the Timber Mountain area on the western boundary of the NTS, separating Pahute Mesa from Yucca Mountain.

SAMPLING METHODOLOGY

Wells sampled at the NTS during FY 92-93 are shown in Fig. 3. The majority of the wells available for isotopic sampling are concentrated in Yucca and Frenchman Flats on the eastern side of the NTS proximal to areas of nuclear testing. A good, but less dense, well coverage exists in the northwestern portion of the NTS on Pahute and Rainier Mesas. Little coverage exists in the west-central area of the NTS. Over half of the wells sampled were drilled at least 25 years ago (Table 1). The depth range among the wells sampled is between 566 to 1675 meters below the surface. Most sampling depths approximately correspond to the depths that the casing is completed, while a few samples were obtained tens to hundred of meters below the completed casing and others within the casing interval. About 25% of the wells sampled have total drill depths that exceed

the groundwater sampling depths by more than 150 meters (Table 1). Most of the total drill depths of the well were not field checked but determined by well history records (Raytheon, 1990). Caving of the lower portion of the wells may occur, but was not specifically investigated in this study.

Both pumped wells and open holes were sampled for isotopic analysis during the FY 92-93 field seasons. Pumped wells are those that provide a steady supply of water at the NTS and are indicated in Table 1. Sampling of the pumped wells entailed a small diversion of the groundwater from the discharge pipe leading from the pump, usually along a point previously developed for water quality sampling or as close to the well head as possible to prevent any contamination along the flow path. Most open holes sampled are covered at the top to prevent foreign material from entering the well bore. On two occasions wells were encountered that were contaminated beyond usefulness: UE-1-L had a substantial amount of diesel fuel on top of the water column, and at well UE-11a extensive organic contamination (dead animal?) was discovered to have altered the groundwater beyond use.

Open holes were sampled using a wireline mechanism and a raised boom (Fig 2). The wireline and raised boom are separate vehicles operated by LLNL at the NTS. Some wells were temperature logged prior to sampling (Table 1). Temperature logs were completed by lowering a calibrated thermocouple tool slowly through the water column at ~3 meters per minute. From the temperature logs, the desired sampling intervals were determined usually based on any occurrences of sharp temperature changes. Where no temperature changes were apparent, the sample was usually collected from the lower half of the well bore, and each sample depth is indicated in Table 1.

For sampling, a remotely controlled valve attached to the wireline tool electronically opened and closed a valve that permitted the evacuated stainless-steel bailers to be filled. This same tool also recorded depth to water in each well. Individual bailers have 2.2 liter volumes with screw-cap ends and O-ring seals equipped with a

needle valve that opened and closed manually. For each sampling of the open hole, two 2.2 liter bailers were attached in line by a brass connector similar to the screw-cap ends, but allowed transmission of water between the two bailers. Each bailer was cleaned with isopropyl alcohol before each drop, attached to the wireline tool, and evacuated to approximately 10^{-2} torr. All needle valves were left open except for the bottom one which was plugged. The wireline and bailers were dropped down the open hole and the water table level was "tagged" before the final depth was reached. The valve in the wireline tool was opened at the predetermined sampling interval by an electronic signal through the wireline and left open for approximately 2-10 minutes. The tool valve was then closed and the bailer was brought to the surface. At the surface, the remaining needle valves were closed, the bailers were detached from the tool and separated into the 2.2 liter sections where they were carried into the field trailer.

During FY 93, an enclosed field trailer was used to process samples. In FY 92, samples were filled in bottles next to the boom truck and field measurements were usually done in a field vehicle or in the back of a pickup truck. The likelihood of significant contamination during the less ideal sampling condition of FY 92 is low and does not seem apparent from the data in Table 2 with the possible exception of well UE-1a which has the highest ^{14}C abundance and is slightly anomalous. Sample bottles were filled directly from the bailers according to the methods outlined in Appendix 1, simultaneous to the field measurements (Table 2). Temperatures were measured as soon as possible after the bailer arrived at the surface, but many measured temperatures maybe greater than the actual down-hole temperatures due to re-equilibration during transport to the surface and handling of the bailers. Sulfate and chloride were measured by ion chromatography at LLNL. Alkalinity was measured by field kits (Hach, and Bausch and Lomb), and comparison of different brand names shows some systematic discrepancy between results, and large uncertainties (± 50 mg/L) arose to their absolute values, particularly during FY 92. Subsequent laboratory extraction of dissolved carbon for ^{14}C

analysis liberates the total dissolved inorganic carbon and the field results were compared against the extraction yields. Where large discrepancies occurred or when field alkalinity was not measured, the extraction yield is reported and noted in Table 2 instead. The dissolved oxygen (DO) was also measured using field kits. Some error may exist in the DO since the rate that oxygen dissolves in an undersaturated sample is rapid relative to the field analytical time, and the water samples in some cases experience a significant exposure (≤ 1 min) to the atmosphere. The pH, total dissolved solids, and specific conductivity were measured using an electronic field measuring instrument calibrated at each new well site. Calibration for pH was against pH 7 and pH 10 buffers and for conductivity against air (zero value) and a 1413 µS standard.

Procedures for filling bottles are listed in Appendix 1 where a step-by-step method was developed specifically for isotopic samples. Analytical procedures for the isotopic analyses in groundwater performed at the Nuclear Chemistry Division of LLNL are listed in Appendix 2

RESULTS AND DISCUSSION

Field data

Water levels in the wells are essentially bimodal with approximately 50% ranging between 700 and 900 meters above sea level, and with the exception of one well, the remainder range between 1100 and 1450 meters above sea level (Fig. 4). An upper horizontal field is defined in Fig. 4 and appears to be related to wells that are drilled on Pahute Mesa. On the Mesa, water tables have higher elevations. The lower horizontal field in Fig. 4 corresponds to wells in the Yucca and Frenchman Flats, where water tables have lower elevations. A non-trivial relationship between the water elevation and the total penetration depth of the wells exists (Fig 4). Under ideal hydrostatic conditions in a groundwater basin, a direct relationship should exist between the water height and the total penetration depth such that,

$$P = \rho g h$$

where P is the overlying pressure exerted on a mass of fluid, h is the height of the fluid column above a datum, ρ is the density of the fluid, and g is the acceleration of gravity. In Fig. 4, the two horizontal fields are indicative of water masses under more hydrostatic conditions, where groundwater from different penetration depths experience different but proportional overlying pressures that essentially maintain a consistent water table among wells. Wells that appear to depart from this relationship are circled in Fig. 4. This field of data preferentially occurs in wells at surface elevations from 1220 to 2070 meters. These wells suggest that the overlying pressure is abnormal causing either sub-normal or artesian conditions relative to the horizontal fields of data. This may be linked to the relationship seen in Fig. 5, where in many cases the change in the surface elevation among wells is greater than the corresponding change in the water table elevations. Figure 5 suggests that the rate of change in the topographic elevation exceeds the rate of change in the water table elevation. As a result, many groundwaters may have sub-hydrostatic pressure gradients relative to depth. This result was derived through observations by Winograd and Thordarson (1975) and Blankennagel and Weir (1973) where perched aquifers and downward fracture flow were shown to exist in some areas of the NTS.

Figure 6 is a map of the wells sampled at the NTS during FY 92-93 plotted with the temperatures of the waters in °F. Some of the geographic variation in the water temperatures is due to the different depths of sampling. The temperature variation in the eastern part of Yucca Flat though, is controlled by locally elevated subsurface temperatures whose anomalies have been noted by previous workers (Thompson, 1991). In an attempt to understand some of the anomalous temperatures, a northwest-southeast cross-section was constructed that shows well depths and contoured temperatures (Fig.

7). The cross-section indicates an anomalously high temperature gradient between wells TW-B and ER-6-1, where a >20°F temperature change occurs across approximately 1830 horizontal meters (0.33°F/100 feet). This same high temperature anomaly has been acknowledged by several other agencies working at the NTS (LANL, USGS and RSN), but detailed studies are lacking. Thompson (1991) documented a substantial increase in subsurface temperatures in southeast Yucca Flat noting vertical temperature gradients from 0.7 to 3.6°F per 100', and postulated a possible structural control on the heat distribution. Similar temperature anomalies have been reported by Blankennagel and Weir (1973) in the eastern Pahute Mesa area where they attributed the elevated temperatures to latent heat from a Tertiary igneous intrusion approximately 2400 meters below the surface. Proper representation of the temperature anomalies in Fig. 6 would require information on the down-hole temperature gradients, and at this time adequate information is lacking and calculation would be crude at best.

The specific conductivities of the groundwaters sampled at the NTS range between 170 and 1300 µS representing typical fresh water concentrations in similar aquifers. The increase in the specific conductivity of ~8 times is mostly controlled by the increased bicarbonate concentrations.

Most of the pH values of the groundwaters range between 6.5 and 9.3. The waters with pHs above 8 typically have higher sodium concentrations and lower bicarbonate concentrations. Even higher pHs occur in the post-shot holes drilled into test cavities and also sample U12s, which is an unused emplacement hole for nuclear testing.

Dissolved oxygen contents in the sampled NTS groundwaters range from approximately 2 to 6 mg/L (Table 2). These values are typical of those noted by other workers (Winograd and Robertson, 1982) in southern Nevada, where the non-zero DO values are attributed to the oxidized volcanic deposits of the NTS and arid vadose zones that lack significant microbial activity available to deplete the DO in recharging groundwaters.

Hydrochemistry

Listed in Table 2 are the major and some minor dissolved constituents in the NTS groundwaters measured during FY 92-93. Dissolved HCO_3 is the dominant anion in all the groundwaters, ranging from approximately 100 mg/L to 500 mg/L with the exception of water supply well UE-19-c that has a concentration of 37 mg/L. Most of the highest HCO_3 wells are completed in the Paleozoic carbonates. The SO_4 concentrations in the samples range between 2 mg/L and 100 mg/L, although the data set in Table 2 is not complete and some higher concentrations in other wells have been reported by previous workers (Winograd and Thordarson, 1975; Chapman and Lyles, 1993). Chloride concentrations usually are low, between 3 and 45 mg/L and do not represent a major control on the total dissolved concentrations of these groundwaters.

Sodium is typically the cation with the highest dissolved concentration in the groundwaters at the NTS and ranges between 30 mg/L and 130 mg/L. The higher Na concentration occurrences are thought to be a result of groundwater flowing through alluvial and tuff dominated aquifers (Winograd and Thordarson, 1975). The Ca concentration of these groundwaters is slightly less than Na and ranges from 1 mg/L to 110 mg/L. The Ca is proportional to the less abundant Mg concentration, whereas the Na is proportional to the less abundant K concentration. The proportional abundance between Na and Ca is almost exactly equivalent to the proportional abundance between Na+K and Ca+Mg (Fig. 8). This relationship suggests that the Na and K have the same source (volcanic rocks) and likewise the Ca and Mg have simialr rgins (Paleozoic carbonates).

Figure 9 is a Piper plot of the major chemical constituents from Table 2. As seen from the figure, the data plot near the HCO_3 apex of the anion triangle with minor deviations toward SO_4 and Cl . The points plotting along the Cl-HCO_3 axis are for samples for which SO_4 data are unavailable. The cation triangle shows a near-linear mixing trend between a Na dominated end-member and an end-member with near equal

proportions of Ca and Mg. The distribution of data in Fig 9 is characteristically similar to Piper plots of chemical data found in Winograd and Thordarson (1975) and Chapman and Lyles (1993), and validates, on the first order, the quality of the major chemical data in Table 2. In detail, the ion balance calculation of the major chemistry shows up to 20% deviations from unity in charge balance between cations and anions, that is probably attributable to analytical error, but represent only minor deviations from the true geochemical character of the groundwaters.

A summary of previous work and a discussion on the origin of the dissolved constituents in the groundwater in and around the NTS is presented in Winograd and Thordarson (1975) where, based on an earlier report by Schoff and Moore (1964), they characterize the groundwater into three catagories: 1) a Na+K-HCO_3 groundwater usually found residing in rocks dominated by volcanic tuff, 2) Ca+Mg-HCO_3 groundwater typically found in the carbonate lithologies, and 3) a groundwater that is a mixture of types 1 and 2. The latter is typically found in many areas of the NTS and has been hypothesized to represent a mixture between the downward flow of groundwater primarily from the volcanic tuffs and the regionally flowing groundwater residing in the Paleozoic carbonates (Winograd and Thordarson, 1975). Flow directions were inferred from the geochemical patterns. Low sodium groundwater is thought to originate in the Pahranagat Valley area and acquire a higher sodium concentration due to both dissolution of minerals along its southeasterly flow path and mixing with groundwater migrating downward from volcanic aquifers (Winograd and Thordarson, 1975).

The Na/Ca weight ratios are listed in Table 2 and range between 0.5 and 43. Weight ratios of Na to Ca measured in rocks of the Paintbrush volcanic tuff (Knauss, 1984) is approximately 4.0 and is probably representative of the elemental ratios in many volcanic tuffs at the NTS, although further research is necessary. The Na/Ca ratios in the groundwaters deviate considerably from the ratios of the host volcanic material. Possible controls on the Na/Ca ratios of the groundwater that exceed 4.0 include: 1) ion exchange

between Ca and Na in clays, 2) differential build up of Na over Ca due to vadose zone evaporation and concentration of salts, 3) and lithological and mineralogical heterogeneities along groundwater flow paths. Processes that might cause the Na/Ca ratio to be lower than 4.0 are 1) dissolution of Paleozoic carbonate material in the bedded aquifers or alluvium dominated by carbonate clasts, and 2) possible lithological and mineralogical heterogeneities with greater susceptibilities for Ca dissolution. Future work that considers all these options will require a more complete understanding of the elemental and mineralogical distribution in NTS lithologies and chemical equilibrium modeling to constrain possible reactions that control the elemental abundances in the groundwater.

Recently, Chapman and Lyles (1993), in a geographically more detailed analysis of the major chemistry in well waters of the NTS, showed that significant heterogeneity exists in the major chemistry among wells considered part of the same flow regimes, particularly in the Yucca Flat and Pahute Mesa areas. Their work demonstrated the scale dependency on the interpretation of mixing and flow in the NTS area using geochemical data. The larger scale geochemical study from which Winograd and Thordarson (1975) derived their flow interpretations probably dampen many of the smaller scale chemical heterogeneities in the groundwater observed by Chapman and Lyles (1993). At the smaller scale, the influence of local geochemical reactions will have a greater bearing on the interpretations of the flow paths.

According to Drever (1988), the aqueous geochemistry of an advecting groundwater mass follows the differential relationship such that,

$$\frac{\partial c_i}{\partial t} = D\frac{\partial^2 c_i}{\partial x^2} - u_x\frac{\partial c_i}{\partial x} + J \qquad (1)$$

where c_i is the concentration of the i_{th} species, D is a diffusion or dispersion coefficient of the particular geologic medium, u_x is flow rate in the x direction, and J is the addition or

loss of dissolved constituents from chemical reactions in the system. The first and third term on the right side of this equation both contribute to the geochemical character of a groundwater. The magnitude of a geochemical effect from the first and third term depends on their comparative rates relative to the fluid flux. The possible influence on the fluid geochemistry from a dominant diffusion and dispersion parameter depends on the porosity and permeability conditions in the aquifer and concentration gradients, where in many cases it has been demonstrated to exert a significant control (see Domenico and Schwartz, 1990 for examples, and also Hendry and Schwartz, 1988). The term *J* dictates the change in the geochemistry due to processes such as adsorption equilibria, chemical equilibration with solids, kinetic reactions of dissolution and precipitation, ion exchange, and in the case of isotopic systems, radioactive decay (Drever, 1988). Areas of lower flow rates can be expected to be influenced greater by the *J* term, than areas where the advection rates are much higher. Interpretations of flow directions based solely on increases of soluble chemical species in the groundwater may be inaccurate, particularly where the groundwater flow rates are much slower than the kinetic rates of chemical reactions between the groundwater and the host rock. Furthermore, pervasive lithological heterogeneties within the NTS complicate interpretations of the observed elemental variation in the groundwater. Flow path histories may be complicated by a groundwater's interaction with one or more host lithological types. This is also an important concept for the interpretation of the environmental isotopic data discussed below.

Environmental Isotopes

Carbon Isotopes - Carbon-14 is a commonly used age discriminator of groundwater ($T_{1/2}$=5730 years; see Mazor, 1991 for review) and provides in many cases the most reliable chronometer for groundwater flow. The ^{14}C is produced by cosmic ray interaction with nitrogen ($^{14}N + n = {}^{14}C + p$) in the upper atmosphere. The ^{14}C derived from atmospheric fallout is incorporated into the dissolved inorganic and organic phases

of the shallow subsurface and decays from an initial concentration that is assumed to be characteristic of a groundwater's recharge area. The ^{14}C abundance relative to the total carbon at any given time is a function of its decay rate such that,

$$^{14}C_{fmc} = e^{-\lambda t} \qquad (2)$$

where $^{14}C_{fmc}$ is the ratio of the measured ^{14}C atomic abundance to an initial abundance, reported as a fraction of modern carbon (fmc), λ is the decay constant, and t is time. The $^{14}C_{fmc}$ is analogous to the more familiar ratio of A/A_0, where A is the measured ^{14}C beta activity in a sample and A_0 is the assumed initial ^{14}C activity of a groundwater mass at the time it was first isolated from the atmosphere. The $^{14}C_{fmc}$ represents a calculated ratio of the ^{14}C atomic abundance of a sample to the ^{14}C atomic abundance of a standard (in this case NBS Oxalic Acid-1) following the derivations of Stuiver and Polach (1977). The $^{14}C_{fmc}$ values in Table 2 do not incorporate any corrections that account for the actual initial ^{14}C abundances in the recharge groundwater mass, but rather all values assume that the initial ^{14}C abundance of the groundwater reflects pre-nuclear testing atmospheric CO_2. Differences between the true initial ^{14}C abundances and the assumed value, and the influence on the measured ^{14}C abundances from subsurface exchange are discussed below. In addition, the $^{14}C_{fmc}$ values have been converted to percentages ($^{14}C_{pmc}$) in Table 2.

The ^{14}C abundances show a range between 1% and 60% modern carbon (Table 2). All the NTS wells appear to have some measurable activity. Over half the wells so far analyzed in Table 2 have ^{14}C concentrations between 1% and 10% modern carbon; UE-1-a alone has an unusually high abundance of 60%. Other workers (Grove et al., 1968; Winograd and Pearson, 1976) have found comparable ^{14}C abundances in the NTS wells, and these and additional measurements are summarized in Spencer (1990).

Apparent ages calculated from the $^{14}C_{fmc}$ are listed in Table 2 and can be considered maximum groundwater ages.

The dissolved ^{14}C abundance of groundwater to the total dissolved carbon varies due to water-rock exchange with ^{14}C depleted carbon-bearing lithologies. This is particularly important for the NTS where the Paleozoic carbonates present a large source of "dead" dissolved inorganic carbon in the vadose and saturated zones. Carbon-13 analyses of the groundwater have been used in an attempt to delineate the different carbon sources at the NTS (Grove et al., 1969; Spencer, 1990). Dissolved inorganic carbon from the root zone of a recharge area usually has a lower ^{13}C abundance (-25.0 to -12.0 ‰, normalized to PDB standard) relative to the Paleozoic carbonates (-2.0 to +2.0 ‰). A mass balance calculation between the two carbon sources has been proposed for the NTS (Grove et al., 1969; Spencer, 1990) which provides a correction factor that is a ^{13}C-dependent ratio such that:

$$^{14}C_{correct} = \left(\frac{\delta^{13}C_{soil} - \delta^{13}C_{carbonate}}{\delta^{13}C_{measured} - \delta^{13}C_{carbonate}} \right) {}^{14}C_{measured} \qquad (3)$$

where $\delta^{13}C = (R_{sa}/R_{st} - 1)1000$, and R is the $^{13}C/^{12}C$ ratio of the sample and a standard respectively. For this equation to be valid for all the groundwaters, 1) a uniform $\delta^{13}C_{soil}$ value is required, 2) the $\delta^{13}C$ increase must be attributable to progressive dissolution of the Paleozoic carbonates, 3) and diffusion and dispersion effects must be negligible. Spencer (1990) suggested that most ^{13}C values for soil carbon at the NTS was -12.0‰, but the latter two requirements have not been addressed to date.

Figure 10 is a $\delta^{13}C$-$^{14}C_{pmc}$ compilation of many springs and groundwaters at the NTS. For equation (3) to be true in all cases, all the $\delta^{13}C$-^{14}C values of groundwaters in Fig. 10 must have a single origination point where the $^{14}C_{pmc} \sim 100$ (assuming 100% initial concentration), and the $\delta^{13}C \sim -12$‰. From this origination point, the $\delta^{13}C$ and

^{14}C values change within a triangular region confined by a line extending from the originating point to $\delta^{13}C = 0‰$ and $^{14}C = 0$. This line defines the change in ^{14}C abundance of a groundwater from dissolution of Paleozoic carbonate with no associated radioactive decay of the ^{14}C, and defines an upper graphical limit on the position of the data points. The data set for the NTS groundwaters in Fig. 10 appears to be confined below this limiting condition. Older groundwaters (<50 pmc) with low $\delta^{13}C$ values suggest that little interaction with the Paleozoic carbonates has occurred, particularly in the Pahute Mesa area. On the other hand, groundwaters with higher $\delta^{13}C$ values suggest a significant interaction with the Paleozoic carbonates.

Figure 11 characterizes the possible pathways that the ^{13}C and ^{14}C abundances in the NTS groundwaters might follow over time. Some of these pathways might cause large uncertainties in the calculated ages. Most groundwaters will originate with a low $\delta^{13}C$ value and a relatively high ^{14}C abundance, possibly near the upper left hand corner of Fig. 11. Lower initial ^{14}C abundances are highly likely (to 50%?) in some cases and their origins would fall below the upper left hand corner. Subsequent ^{14}C decay and dissolution of the Paleozoic carbonates will cause a migration along some near exponential decay pathway that trends toward a 0‰ $\delta^{13}C$ value and a 0% ^{14}C concentration. Dispersion and diffusion of the carbon isotopes within the aquifer will accelerate this trend along a similar pathway, but probably only represent a minor effect. A vertically downward pathway may occur if dissolution of the Paleozoic carbonates is negligible and only ^{14}C decay occurs. Some groundwaters may originate with higher initial ^{13}C concentrations in the vadose zone and the subsequent decay pathways may be shifted to the right. Overall, the carbon isotope evolution of all the groundwater influenced by the Paleozoic carbonate will define a broad curvilinear zone that progresses to zero values for both isotopic systems. Isotopic equilibration between the groundwater and the host rock will be more progressive for older waters, and the broad band defined in Fig. 11 should narrow as it approaches the zero isotopic values. This latter effect is

clearly seen in the NTS data of Fig. 10. Precipitation and dissolution of the dissolved bicarbonate and decay of ^{14}C are probably the main controls on the carbon isotope values of the NTS groundwaters.

Specific examples of uncertainties that arise in the carbon isotopes can be seen in some of the data points in the lower right hand corner of Fig. 10. For instance, well UE-18-r has a ^{14}C abundance of 8% and a high $\delta^{13}C$ value of -1.4‰, even though the well is completed in the volcanic tuffs. Such high ^{13}C concentrations would be expected for groundwater in the Paleozoic carbonate aquifer, and is uncharacteristic of residence in volcanic material where carbon sources are limited. There is no evidence thus far that suggests the groundwater in UE-18-r may originate from the Paleozoic carbonates. More likely, the initial $\delta^{13}C$ value of the groundwater that recharged UE-18-r was high, and its subsequent ^{14}C decay pathway has been vertically downward from the upper right hand corner of Fig. 10 to its present position.

Two groundwaters plotted in Fig. 10 (UE-1q and ER-6-1) are from wells completed in the carbonates drilled by the Groundwater Characterization Project. They have ^{14}C abundances of 7.7 and 2.1% respectively, and $\delta^{13}C$ values of -2.3 and -0.7‰. The ^{13}C content of the groundwater from these wells is very close to typical values in the Paleozoic carbonates. Both of these wells are cased down to the Paleozoic carbonates below Yucca Flat and the carbon isotope data suggest that the water has seen a significant residence time within these rocks. Applying equation 3 to these groundwaters would result in corrected ages between 7600 and 8600 years as compared to 20,650 and 32,100 years for apparent ages. Extensive isotopic exchange of ^{13}C between the groundwater and the carbonates is plausible, which would cause an increase in the $\delta^{13}C$ values of the groundwater and a net decrease in the ^{14}C atomic abundance, but not necessarily an increase in the dissolved bicarbonate. Use of equation 3 depends on the coupling between the change in $\delta^{13}C$ of the groundwater with the increased dissolved bicarbonate due to dissolution. Therefore, the corrected ^{14}C ages of this groundwater would represent

a minimum residence time. The actual ages of this groundwater lie between the corrected ages and the apparent ages derived from the raw data (Table 2), leaving at this time a high uncertainty. More detailed laboratory and field analysis will narrow the possible age range of many of these groundwaters.

Chlorine-36 - Several studies have attempted to exploit the natural radioactive decay rates of ^{36}Cl ($T_{1/2}$ = 301,000 yrs) for age dating of old groundwater (see Bentley, 1986). Chlorine-36 is produced in the upper atmosphere by spallation of argon-40 by high energy protons and neutron capture by argon-36 (Davis and Murphy, 1986). Steady-state fallout of the ^{36}Cl atoms from atmospheric circulation and dissolution into precipitation provides a constant supply to the total atmospheric chloride. Above-ground nuclear testing released a large anthropogenic pulse of ^{36}Cl to the atmosphere beginning in the late 1950's, and has returned to near-natural levels at present time. Aerosols provide chloride from the sea that have undetectable ^{36}Cl concentrations, and dilutes the $^{36}Cl/Cl$ ratio in precipitation. The dilution causes a gradient in the $^{36}Cl/Cl$ ratio in average precipitation with increasing $^{36}Cl/Cl$ contributions occurring toward the continental interior (Bentley, 1986). In principle, the initial ^{36}Cl atom abundance in young groundwater is indicative of the average ^{36}Cl atom abundance of local precipitation in the groundwater's recharge area. Most groundwaters in the unsaturated and saturated zones have chloride concentrations much higher than those measured in precipitation (Bentley et al., 1986), where evaporative concentration effects in the unsaturated zone increase the total dissolved chloride by at least an order of magnitude. Bentley et al. (1986) observed the evaporative effects on the ^{36}Cl atom concentration in the recharge groundwaters of the Great Artesian Basin, where, because the ^{36}Cl atom concentration is measured relative to a fixed volume, the evaporative concentration decreases the volume of water in the unsaturated zone and proportionally increases the ^{36}Cl atom concentration in the

water. Many workers report ^{36}Cl values as a ratio to total chloride since the ratio does not change during evaporation.

Norris et al. (1987) and Phillips et al. (1988), tracing bomb pulse ^{36}Cl and tritium in the vadose zone, have both shown that chloride mobility (and hence ^{36}Cl mobility) in the upper vadose zone (~2m) is much slower than water, due to phase relations that transport water as a liquid and a vapor, where chloride movement is limited only to the aqueous phase. The chloride distribution and mobility in the vadose zone is spatially heterogeneous (Norris et al., 1987) possibly due to differing infiltration rates.

Bentley et al. (1986) first applied ^{36}Cl dating methods to the Great Artesian Basin in Australia, where they showed systematic age increases (from <100,000 to 1,200,000 yrs) with increasing depth along a Jurassic sandstone aquifer. These ages agreed with hydrodynamically calculated ages. Bentley et al. (1986) further proposed that the natural decay of ^{36}Cl is partially countered by simultaneous production of ^{36}Cl in the subsurface due to neutron flux from other radioactive elements (e.g. uranium). Phillips et al. (1986) attempted to apply the same principles to the Milk River aquifer in Alberta, Canada, where a non-systematic trend in the ^{36}Cl atom abundance was interpreted to be influenced by ion filtration of chloride in the subsurface. Based on this assumption, Phillips et al. (1986) calculated ages from 500,000 to 2,000,000 yrs for the groundwater. Subsequent works (Hendry and Schwartz, 1988; Nolte et al., 1991; Fabryka-Martin et al., 1991) have demonstrated that groundwater dispersion and chloride diffusion are probably controlling the ^{36}Cl atom abundances in the Milk River aquifer rather than ion filtration, and maximum ages may only be 1,000,000 yrs, although these ages are still a factor of two greater than the calculated hydrodynamic ages. Recently, Andrews and Fontes (1993) questioned the validity of dating of very old groundwater with ^{36}Cl, calling attention to the predominance of "dead" chloride in the deeper groundwaters and simultaneous increase in the chloride concentration. Radioactive decay of ^{36}Cl is slow compared to chronometers such as ^{14}C, and its use as a groundwater age indicator

requires water of a considerable age. All groundwater at the Nevada Test Site has some level of ^{14}C activity, and any depletion of an initial ^{36}Cl abundance due to decay would be less than 2% and age discrimination using ^{36}Cl is improbable (Davisson et al., 1993). This report will focus, on the other hand, on the sources of chloride and ^{36}Cl variations in saturated zone groundwaters at the NTS, and interpret the ^{36}Cl data and discuss their evaporative concentration effects in the vadose zone.

The $^{36}Cl/Cl$ ratios in Table 2 show that a large variation exists in the groundwaters sampled at the NTS. Most groundwaters have ratios between 100 and 1000 x 10^{-15} with many occurring in the middle of this range. The ^{36}Cl atom concentrations per volume range from 3.6 to 38.6 x 10^{7} atoms/L and mimic the order of magnitude variation of the $^{36}Cl/Cl$ ratios, although most atom abundances range between 5 and 17 x 10^{7} atoms/L. One sample has an unusually high abundance (UE-5n) attributed to contamination. UE-5n (^{3}H = ~3100 TU) is a near-by satellite well to the Cambric Ditch, which contained radionuclide enriched fluids pumped during an induced radionuclide migration experiment from the Cambric cavity (Bryant, 1992). Subsurface migration from the ditch to UE-5n probably has occurred over the subsequent time (Buddemeier et al., 1991).

Aside from well UE-5-n, the range in $^{36}Cl/Cl$ ratios of the sampled groundwater is similar to ratios measured in soil (500 x 10^{-15}) about a meter below the surface (below the bomb pulse) as determined by other workers in unsaturated zone studies at the NTS (Norris et al., 1987). With the exception of wells WW-C, WW-C1, and UE-1h little change in the $^{36}Cl/Cl$ ratios has occurred between the unsaturated zone and the saturated zone, although a significant variation exists in terms of the calculated ^{36}Cl age ($\leq$ 285,000 years). The three wells listed above as exceptions appear to be around a factor of two to six lower than most other wells in their $^{36}Cl/Cl$ ratios, but due to their abnormally high Cl concentrations, fall within the same range of the other wells in their ^{36}Cl atom abundances.

Figure 12 is a plot of the $^{36}Cl/Cl$ ratios of groundwaters from the NTS and the Dakota Aquifer in Kansas plotted against the log of their Cl concentrations. The concept of this graphical relationship first purposed by Andrews and Fontes (1993) demonstrates the evaporative enrichment of Cl in the vadose zone and the subsequent mixture with "dead" Cl in the saturated zone. Evaporative enrichment is best seen on the upper portions of the diagram where the $^{36}Cl/Cl$ ratios are above 1000 and the Cl concentrations vary between 2 and 50 mg/L. Here the net evaporation of vadose zone water causes differential increases in the total Cl concentration per unit volume, but has no effect on the $^{36}Cl/Cl$ ratio. The net effect in the upper portion of the data on this plot is to cause a wide variation in Cl concentrations but a negligible variation in the $^{36}Cl/Cl$ ratios. This same effect can be seen in the NTS groundwater data as well.

Both the Dakota aquifer and NTS groundwaters decrease their $^{36}Cl/Cl$ ratios and increase their Cl concentrations due to the influence of "dead" subsurface Cl on the absolute ratios in the groundwater. For instance, the groundwaters from the Dakota aquifers significantly increase their chloride concentration with depth and confinement, where the source of the Cl can be traced to dissolution of evaporites at depth and upward advection and diffusion of the NaCl. The dissolved evaporites have essentially no measurable ^{36}Cl and their dissolution into the overlying groundwater causes a decrease in the net ^{36}Cl abundance in the groundwater. This effect is best seen in the curvilinear trend of the Dakota aquifer data towards higher Cl concentrations and lower $^{36}Cl/Cl$ ratios (Fig. 12). To a lesser extent, the NTS data also shows a tendency toward higher Cl concentrations with a corresponding decrease in its $^{36}Cl/Cl$ ratios. The subsurface source of Cl at the NTS is not readily apparent at this time and may be attributable to residual marine Cl in the Paleozoic rocks, as well as contribution of Cl from the host lithology during dissolution as the groundwater increases in age. Further investigation is still required, but it is useful to note that the lowest $^{36}Cl/Cl$ ratios in Table 2 are derived from

wells that are predominantly completed in the Paleozoic carbonates and where marine sources of "dead" Cl appears most plausible.

Strontium Isotopes - Strontium dissolved in groundwater acquires the $^{87}Sr/^{86}Sr$ isotopic signature of its host aquifer. The $^{87}Sr/^{86}Sr$ ratio does not mass fractionate under the physical conditions experienced by groundwater, and therefore can potentially trace water-rock reactions and mixing of isotopically distinct waters. An increasing $^{87}Sr/^{86}Sr$ ratio may be indicative of sources with higher Rb/Sr ratios (^{87}Rb decays to ^{87}Sr; half life= $4.8x10^{10}$ years).

Sr isotopes have been employed at the NTS to specific hydrologic investigations relating to the vertical movement of the water table at Yucca Mountain (Marshall et al., 1993, Peterman et al., 1992a, Stuckless et al., 1991), but only Peterman et al. (1992b) have proposed a comprehensive regional model of hydrologic flow using these isotopes. They determined that recharged groundwater in the Spring Mountains has a $^{87}Sr/^{86}Sr$ ratio ranging between 0.70845 and 0.70976 that is similar to a 0.70845 mean Sr isotopic ratio for the carbonate rocks through which this recharge occurs. Inflow from the Pahranagat Valley ranges from 0.71079 to 0.71392, representative of ground-water signatures of the regional carbonate aquifer comprising southern Nevada. The $^{87}Sr/^{86}Sr$ values of discharge along the line of springs in Ash Meadows in the Amargosa Valley southwest of NTS range from 0.71234 to 0.71905, where the more radiogenic waters represent an anomalously high $^{87}Sr/^{86}Sr$ input to the southern end of the spring line. Well waters sampled from the east central part of the NTS from the regional carbonate aquifer have $^{87}Sr/^{86}Sr$ values between 0.71272 (well UE-7NS) and 0.71489 (well C-1). Peterman et al. (1992b) conclude that the radiogenic signatures observed in the west-central part of the flow system and from the Pahranagat Valley balance the less radiogenic signatures of recharge in the Spring Mountains and produce, through mixing, intermediate values for the spring discharge in Ash Meadows. The source for the

extremely radiogenic water flowing from the northern extremities of the Ash Meadows system is not identified, but they suggested that such signatures would be derived from radiogenic siliciclastic sources.

To further characterize the Sr isotopic signature of groundwater as a function of the host aquifer's lithology, Peterman et al. (1992b) used Ca/Na ratios of southwestern Nevada groundwater to distinguish the volcanic from carbonate aquifers. The Ca enrichment in the water is derived from dissolution of carbonate aquifers, while they believed that Na is enriched by dissolution of the Tertiary silicic volcanic aquifers. They found that the Ca/Na ratio inversely correlates with the $^{87}Sr/^{86}Sr$ ratios of the groundwater. Similarly, though, a plot of Ca verses Si for the HRMP data (Fig. 13) indicates two distinct trends. Ca is enriched relative to Si for waters derived from wells exclusively producing from the carbonate aquifer. In contrast, Si is enriched relative to Ca in waters derived both from wells producing solely from the volcanic aquifer and from wells producing from the volcanic and the underlying carbonate aquifers. The corresponding $^{87}Sr/^{86}Sr$ ratios adjacent to the data points in Fig. 13 demonstrate that a radiogenic source of Sr is derived from carbonate bearing lithologies and not only radiogenic siliciclastic sources as suggested by Peterman et al. (1992b). Fig. 14 further suggests that the enriched $^{87}Sr/^{86}Sr$ ratios correspond to elevated HCO_3 concentrations. Aside from Sr isotopic zonation that occurs in the volcanic tuffs (Stuckless et al., 1991), a strong possibility exists that more radiogenic sources of Sr occur in the Paleozoic carbonates and that $^{87}Sr/^{86}Sr$ heterogeneities must be accounted for before simple conclusions on groundwater flow are drawn from the Sr isotope data. In particular, an investigation of the role of secondary mineralization is needed to determine its effect on the Sr isotope signature of the groundwater.

Uranium Isotopes - To date, no final $^{234}U/^{238}U$ ratios are available from FY 92-93 sampling; although most samples have been analyzed, the results are undergoing data

reduction and review. A brief review of $^{234}U/^{238}U$ is presented below. The final FY 92-93 report will incorporate the yet unreported analyses and build an interpretive framework from the discussion below.

The secular equilibrium of natural radioactive decay established between ^{234}U and ^{238}U have been used to estimate groundwater ages (for review, see Davis and Murphy, 1986). The activity ratio of $^{234}U/^{238}U$ should equal 1.0 when the two isotopes have equal solubility in the groundwater and when ^{234}U and ^{238}U are in secular equilibrium in the host rock. Typically, the activity ratios are greater than 1.0 in many groundwaters. This is due to 1) the greater solubility of ^{234}U from crystal lattice sites damaged from alpha-recoil during decay of ^{238}U, and 2) the alpha-recoil ejection of ^{234}Th (daughter of ^{238}U that decays to ^{234}U) from the crystal lattice. The ^{234}Th has a very low solubility and most likely decays to ^{234}U ($T_{1/2}$ = 24 days) from a solid phase that precipitated after ejection. The ^{234}U subsequently is more soluble than ^{234}Th and its activity increases in the groundwater over the ^{238}U.

Osmond and Cowart (1982) have presented the most comprehensive data base of $^{234}U/^{238}U$ for groundwater and springs in southwestern Nevada (Fig. 15). Because most groundwaters in southwestern Nevada are oxidizing, Osmond and Cowart (1982) suggested that the uranium can be considered a conservative aqueous species. They suggested that the ^{234}U excess of the groundwaters in the carbonate aquifer is controlled by mixing between the recharge areas of the Spring Mountains and the Pahranagat Valley. From their data, they further suggested that the Indian Springs area and the Yucca Flat carbonate aquifer have little contribution to the Ash Meadows discharge (Fig. 15).

GCP wells ER-6-1 and UE-1q are also plotted in Figure 15. As can be seen, the GCP wells do not plot within the mixing triangle suggested by Osmond and Cowart (1982), but rather have a much higher ^{234}U excess. This suggests that the uranium concentrations and the $^{234}U/^{238}U$ activity ratio may have a more local control in Yucca

Flat and do not suitably compare to the regional interpretation Osmond and Cowart (1982). Possible controls on the aqueous uranium may be due to a heterogeneous distribution of uranium in the rock. It may also be possible that a significant variability in oxidizing conditions in the subsurface exists and limits uranium mobility.

Noble Gas - The non-radiogenic noble gas concentrations in groundwater offer a variety of important information on the source and age of a groundwater mass. In particular, Mazor (1972) showed that the temperature dependency of argon, krypton, xenon, and neon solubility in groundwater could be exploited to determine recharge temperatures by accurately measuring the absolute abundances of the noble gases dissolved in the groundwater.

Samples for noble gas abundances were collected during FY 92-93 for all the water supply wells but have not been analyzed to date. These same noble gas analyses have been performed on two GCP wells listed in Table 2. Using well UE-1q as an example, its noble gas abundance suggests a recharge temperature of 16 ± 1°C. This temperature is consistent with current mean annual air temperatures measured within this region of the NTS (Winograd and Thordarson, 1975; Lyles and Mihevc, 1992). Based on an altitude calculation from the noble gas data, a 1500 ± 300m elevation is determined. Yucca Flat elevation ranges approximately from 1200m at the valley floor to 1800m for the adjacent hills, and this elevation range is entirely consistent with the noble gas calculations. In general, the noble gas data are consistent with the idea that the recharge is of local origin, and agree with the ^{14}C results and the conclusions of Winograd and Thordarson (1975).

Because of the long range transport of ^{4}He in the crust, it is difficult to use ^{4}He accumulation as a precise groundwater chronometer. Since the aquifer is a trap for ^{4}He, however, high concentrations of ^{4}He generally indicate long residence ages for the groundwater. A simple model can be used to estimated the residence age. We take a

uniform crustal flux of ^4He to be 3 x 10^5 atoms $^4He/cm^2$ sec (e.g. Torgerson and Clarke, 1985 and O'Nions and Oxburgh, 1983), and given the ^4He flux into the water and the volume of the water, we can calculate the rate at which the ^4He concentration should increase or:

$$^4He = \left(\frac{(Flux)(Residence\ age)}{(Aquifer\ thickness)(Porosity)} \right).$$

The measured radiogenic ^4He concentration is about 10^{12} atoms/ml for UE-1q (Davisson et al., 1993). If we choose an aquifer thickness of 10^3 m and a porosity of 20%, then we calculate an age of approximately 3700 years (This departs from the calculated age given in Davisson et al., 1993 by a factor ten due to a revised ^4He flux). In general, the water is old but the ^4He data gives an age a factor of 6 less than the apparent ^{14}C age. The lower apparent ^4He age may be due to a reduced regional flux of ^4He into the aquifer beneath the Nevada Test Site. This model also assumes that no ^4He loss from the aquifer has occurred. The ^4He age is very uncertain at this time but may be calibrated against the ^{14}C ages as the data base grows.

Contaminant Characterization

Radionuclides - The radionuclides ^3H, ^{60}Co, ^{85}Kr, ^{90}Sr, ^{99}Tc, ^{125}Sb, and ^{137}Cs comprise the suite of radiochemical analyses measured during FY 92-93 that also may include the environmental isotopes ^{36}Cl, ^{14}C, and ^{129}I. These radionuclides are weapons testing-related products commonly found in subsurface nuclear test cavities. Their moderate to long half-lives make them ideal radioactive contaminant tracers of nuclear cavity products. All concentrations for these constituents measured thus far on the HRMP samples, with the exception of ^3H (and the environmental isotopes), are below detectable limits (Table 2). With the exception of one well (UE-5n) measured during FY 92-93, the

^{3}H contents are at natural, non-contaminant levels. In addition, all the levels, including the ^{3}H, are well below the maximum permissible concentrations for potable groundwater. Below is a list of proposed federal drinking water limits of the radionuclides (Federal Register, 1991) measured for this report:

Tritium (^{3}H)	60,000 pCi/L
Carbon-14 (^{14}C)	3200 pCi/L
Chlorine-36 (^{36}Cl)	1850 pCi/L
Cobalt-60 (^{60}Co)	218 pCi/L
*Krypton-85 (^{85}Kr)	250 pCi/L
Strontium-90 (^{90}Sr)	42 pCi/L
Technetium-99 (^{99}Tc)	3790 pCi.L
Antimony-125 (^{125}Sb)	1940 pCi/L
Iodine-129 (^{129}I)	21 pCi/L
Cesium-137 (^{137}Cs)	119 pCi/L
Uranium-234 (^{234}U)	26 pCi/L
Uranium-235 (^{235}U)	27 pCi/L
Uranium-238 (^{238}U)	26 pCi/L

* Value is 10 times the analytical limit and is set by the UGTA RI/FS at DOE Nevada.

Most radionuclide characterization of groundwater at the NTS has incorporated the analysis of water from or near detonation cavities (Borg et al., 1976; Crow, 1976; Bryant, 1992) where fission-related contaminants comprise a radionuclide source term including groundwater and melt glass (Smith, 1993). Radionuclides currently being analyzed for these HRMP samples are common fission products (^{85}Kr and ^{99}Tc), neutron activation products (^{60}Co), or radiogenic products from decay of short-lived fission

products (^{90}Sr, ^{137}Cs, ^{125}Sb, ^{85}Kr, and ^{99}Tc) produced from a subsurface nuclear detonation (Borg et al., 1976; Bryant, 1992). The activity level of any particular one of these radionuclides in the groundwater depends on the magnitude and the type of test and the response of the geologic medium (Borg et al., 1976).

Krypton-85 is in a dissolved gas phase and has a higher rate of mobility within the groundwater than ^{90}Sr and ^{137}Cs which tend to absorb to rock material and be immobile, although their fission product precursors were volatile nuclides with a potential for short range migration. Technetium-99 is mobile in oxidized waters, whereas ^{60}Co and ^{125}Sb tend to have a low mobility and an affinity to rock absorption.

The ^{3}H analyses completed at LLNL are determined using the ^{3}He accumulation technique (Surano et al., 1992). In this method, all the ^{3}He initially present in the sample is removed and the ^{3}H is allowed to decay to its daughter product ^{3}He for a known length of time, and accumulate to a measurable concentration. After about 60 days, the accumulated ^{3}He is analyzed by high sensitive mass spectrometry (detection limit = 10^{4} atoms ^{3}He).

Tritium ($t_{1/2}$=12.43 yrs) is produced in the upper atmosphere by nuclear reactions between energetic cosmic rays and nitrogen and oxygen. This natural production mechanism leads to a mean ^{3}H concentration in continental precipitation of about 5 TU (Craig and Lal, 1961; 1TU = 3.2 pCi/l H_2O = 0.12 Bq/l H_2O).

With the advent of atmospheric nuclear testing, ^{3}H levels in precipitation rose dramatically (especially in the northern hemisphere) to a peak value of about 1000 TU in 1963 (Weiss and Roether, 1980). Current precipitation averages about 10-20 TU in central continental areas and averages about 5 TU near the California coast.

All of the samples analyzed have relatively low to undetectable ^{3}H levels with the exception of UE-5n. This sample shows ^{3}H at 3100 TU, that given its close proximity (~300 meters) to the Cambric ditch, must be receiving infiltrated tritiated water that recharged when the ditch was full during the pumping experiments with the Cambric

cavity (Bryant, 1992). The ^3H value of UE-5n is less than 1% of the Cambric ditch water ^3H activity and is about half the drinking water standard of 20,000 pCi/l (6250 TU). Ruggieri et al. (1988) determined that infiltration rates of tritiated water below the Cambric ditch was approximately 0.3 m/day, or about 110 m/year. The Cambric event pumping experiment was initiated in October 1975 where water discharged from the well into the Cambric ditch reached a maximum concentration of 10^7 pCi/L. Over the course of 18 years since the pumping was initiated, the tritium maximum concentration today would be approximately 3.8×10^6 pCi/L. This tritium pulse would be able to reach the water table in UE-5n at ~215 meters within a minimum of 3-4 years. The tritium concentration in UE-5n is <1% of the expected concentration of the Cambric ditch water. The tritium in UE-5n probably represents a dispersive tail of the tritium plume beneath the Cambric ditch and greater tritium concentrations ($\leq 3 \times 10^6$ pCi/L) may occur adjacent to the well With time, dispersion of the tritium will decrease its total concentration per volume.

About half of the remaining samples show ^3H below 0.5 TU indicating essentially pure pre-nuclear test water. The remainder of the samples show values up to about 4 TU which suggests the presence of some anthropogenic ^3H. However, two duplicate analyses within this set showed variations of this magnitude, so we are concerned that an analytical blank problem might exist (although none of the analytical blanks showed the effect). All of the samples which showed detectable ^3H are being re-analyzed and will be included in the final report.

The Nuclear Chemistry Division has extensive experience with nuclear diagnostic measurements involving hydrogen isotopes. On a large number of underground nuclear explosions (about 20), we have included large quantities of D_2O as a tracer for residual ^3H. From measurements of promptly recovered hydrogen and water, we were able to infer the extent of dilution of the bomb residual ^3H by local groundwater. We were also able to deduce the distribution of residual ^3H between HT (tritiated hydrogen gas) and

HTO (tritiated water). We expect little of the HT to be incorporated into the groundwater mass, while most of the HTO would combine with the groundwater mass. The experimentally determined results show that the majority of the residual ^3H (>95%) ends up as HTO due to isotopic exchange between HT and H_2O at temperatures around 700°C. The mass of the H_2O which equilibrates with the gaseous HT is reasonably constant at two times the water contained in the explosion melt mass or about 10^9 gH_2O/kiloton. For most underground nuclear tests, the water content is about 10-20% by weight (nearly saturated). Thus we can conclude that about 3×10^5 liter of H_2O/kiloton mixes with the device residual ^3H. Device residual ^3H varies considerably but can be estimated on a case by case basis. We have adopted 10^9-10^{10} pCi/l H_2O as an average value for the cavity source term and we believe that the majority of this water is freely available to enter and mix with groundwater. Activity levels detected outside of cavities tend to be somewhat lower (e.g. $^3H=1x10^6$ to $1x10^7$pCi/L, Crow, 1976; Bryant, 1992) due to the groundwater dilution.

Field beta scans of the groundwater sampled in the drill-back holes at the NTS show levels from a factor of 100 less than drinking water levels (UE-7ns) to levels over a factor of 1000 greater than drinking water limits (U-4u). All fall at or below the observed level of tritium outside of cavities mentioned above and suggests that groundwater dilution may have occurred in the zones penetrated by these wells.

SUMMARY

This report presents the initial results and preliminary interpretation for a new geochemical and isotope data base developed for the NTS groundwaters. Techniques for field sampling using wireline bailing methods and utilizing existing pumping systems, as well as analytical procedures for the isotopic analysis have been developed.

Field measurements of water levels in the sampled wells indicate essentially a bimodal distribution separating water levels at higher elevations (e.g. Pahute Mesa) from

water levels of lower elevations (e.g. Yucca and Frenchman Flats). The remaining water levels appear to form a non-hydrostatic transition between the two groupings of water levels and are probably related to higher elevations adjacent to the Flats. Down-hole temperature measurements have confirmed anomalous temperature gradients in the eastern Yucca Flat area and on Pahute Mesa, where horizontal temperature gradients up to 0.33°F/100ft are found.

Consistent with previous work by others, the major ion geochemistry of the NTS groundwater is dominated by Na-K-HCO_3 and Ca-Mg-HCO_3 water types, where the Na-rich water appears to be related to dissolution of the volcanic tuffs and the Ca-rich water is related to dissolution of the Paleozoic carbonates. An increase in dissolved Si also seems to be indicative of groundwater that resides in the volcanic tuffs. The source(s) of the variation of the Na/Ca ratios may be complex and controlled by ion exchange reactions with clays, evaporative concentration in the vadose zone, and lithological heterogeneities in addition to simple differential dissolution between the volcanic tuffs and the Paleozoic carbonates.

To date, ^{14}C measurements on 15 wells yield apparent ages between 4000 and 38,000 years for groundwaters at the NTS. Age calculations at this time have high uncertainties (± 10,000 years on some wells) due to carbonate dissolution and $\delta^{13}C$ variability and exchange. Many of the groundwaters decrease their ^{14}C relative abundance as their HCO_3 concentrations increase suggesting that dissolution of carbonates control the apparent ages. Carbon-13 analysis of the groundwater indicate that isotopic contribution to the dissolved HCO_3 is probably from the "dead" Paleozoic carbonates, consistent with previous reports. Further investigation of the vadose zone carbonate would help to constrain all the potential carbon sources and influence on the ^{14}C atomic abundances in the saturated zone. The uncertainty in the calculated ages will decrease as more geographical and geochemical constraint can be made on: 1) the recharge $\delta^{13}C$ signature of the groundwater, 2) the extent of carbonate dissolution and

isotopic exchange with the Paleozoic carbonates, and 3) the initial ^{14}C atomic abundances in the recharging groundwater.

The $^{36}Cl/Cl$ ratios measured in the NTS groundwaters do not indicate the presence of very old groundwater, in agreement with the observation that all groundwaters have a perceptible ^{14}C activity. The ^{36}Cl systematics have been investigated and compared with similar groundwater conditions in the Dakota Aquifer of Kansas, where it is found that addition of a "dead" ^{36}Cl chloride source to the dissolved chloride in the groundwater lowers the $^{36}Cl/Cl$ ratios by a factor of 10 or more. In the case of Kansas, ^{36}Cl depleted saline brines diffuse upward and mix with the potable groundwater at shallower depths. At the NTS addition of "dead" chloride by perhaps the Paleozoic carbonates and the volcanic tuffs are contributing to much of the decrease in the $^{36}Cl/Cl$ ratios of the groundwater.

Initial results of $^{87}Sr/^{86}Sr$ measurements of the dissolved Sr in the NTS groundwaters indicate that the less radiogenic component is characteristic of higher Si concentrations related to the volcanic tuffs, where more radiogenic values are associated with higher bicarbonate concentrations and the Paleozoic carbonates. Lithological heterogeneities and secondary mineralization may be major controls on the $^{87}Sr/^{86}Sr$ ratios of the NTS groundwaters and further investigations are needed.

The $^{234}U/^{238}U$ values measured in the NTS groundwaters during FY 92-93 are not included in this report and are undergoing data reduction. A review of previous work on $^{234}U/^{238}U$ at the NTS is presented.

Measured noble gas abundances in the water supply wells are anticipated in the near future. The data should yield information regarding the recharge temperatures and elevations of the groundwater. In the future, ^{4}He concentrations may help calibrate the ^{14}C ages .

Contaminant characterization of select fission related radionuclides is in progress for all wells in addition to drill back holes in explosion cavities. Results from tritium

analyses indicate that all wells, with the exception of the drill back wells, fall well below the drinking water standards. Many of the wells are tritium dead indicating old groundwater, where some wells may suggests some anthropogenic levels of tritium of very low levels, but analytical uncertainties are very high at this time and re-analysis is needed. Well UE-5n shows a substantial tritium level of approximately 9900 pCi/L or half the drinking water standard. The tritium source probably originates from infiltration of Cambric ditch tritiated water, and is consistent with fluid rate calculations. Field measurements of tritium levels in the drill back wells vary up to 5 orders of magnitude, with the highest occurring in well U4u at approximately 10^7 pCi/L.

ACKNOWLEDGMENTS

We gratefully acknowledge the indispensable help of John Andrews, Joan Beiriger, Jan Brown, Dick Nagel, Ken Marsh, Sid Niemeyer, Marc Caffee, Bob Finkel, Carol Velsko, and the numerous individuals at the NTS whose knowledge and experience contributed to the success of this project.

REFERENCES

Andrews, J.N. and Fontes, J. Ch., 1993, Comment on "Chlorine-36 dating of very old groundwater, 3, further results on the Great Artesian Basin, Australia" by Torgensen et al. Water Resources Research, 29, 1871-1874.

Bentley, H.W., 1986, Chlorine-36 in the terrestrial environment, in Fritz, P., Fontes, J. Ch., eds. Handbook of Environmental Isotope Geochemistry. p. 427-480.

Bentley, H.W., Phillips, F.M., Davis, S.N., Habermehl, M.A., Airey, P.L., Calf, G.E., Elmore, D., Gove, H.E., Torgersen, T., 1986, Chlorine-36 dating of very old groundwater: 1. The Great Artesian Basin, Australia. Water Resour. Res., 22, p. 1991-2001.

Blankennagel, R.K. and Weir, J.E., 1973, Geohydrology of the eastern part of Pahute Mesa, Nevada Test Site, Nye County, Nevada. USGS Prof. Paper 712-B, 35 pgs.

Borg, I.Y., Stone, R., Levy, H.B., Ramspott, L.D., 1976, Information pertinent to the migration of radionuclides in groundwater at the Nevada Test Site. UCRL-52078, LLNL, 216 pgs.

Bryant, E.A., 1992, The Cambric migration experiment. LA-12335-MS, LANL, 37 pgs.

Buddemeier, R.W., Finkel, R.C., Marsh, K.V., Ruggieri, M.R., Rego, J.H., Silva, R.J., 1991, Hydrology and radionuclide migration at the Nevada Test Site. Radiochimica Acta, 52/53, 275-282.

Chapman, J.B. and Lyles, B.F., 1993, Groundwater chemistry at the Nevada Test Site: Data and preliminary interpretations. Desert Research Institute Water Resources Center Publication 45100, 45 pgs.

Craig, H. and Lal, D., 1961, The production rate of natural tritium, Tellus 13, 85-105.

Crow, N.B., 1976, First observations of tritium in groundwater outside chimneys of underground nuclear explosions, Yucca Flat, Nevada Test Site. UCRL-52073, LLNL, 36 pgs.

Davis, S.N. and Murphy, E., 1986, Dating Groundwater and the Evaluation of Repositories for Radioactive Waste. NUREG/CR-4912, University of Arizona. 181 pgs.

Davisson, M.L., G.B. Hudson, J. Kenneally, G.J. Nimz and J.H. Rego, 1993, Report on the radiochemical and environmental isotope character for monitoring well UE-1q: Groundwater Characterization Program, Lawrence Livermore National Laboratory, UCRL-ID-114158, 28p.

Domenico, P.A. and Schwartz, F.W., 1990, Physical and Chemical Hydrogeology. John Wiley and Sons: New York, 824 pgs.

Drever, J.I., 1988, The Geochemistry of Natural Waters. Prentice Hall: New Jersey, 435 pgs.

Elmore, D., et al., 1979, Analysis of ^{36}Cl in environmental water samples using an electrostatic accelerator. Nature, 277, p. 22-25.

Fabryka-Martin, J., Whittemore, D.O., Davis, S.N., Kubik, P.W., Sharma, P., 1991, Geochemistry of halogens in the Milk River aquifer, Alberta, Canada. Applied Geochem., 6, p. 447-464.

Failoı, R.A., Beiriger, J., Rego, J.H., Buddemeier, R.W., Marsh, K.V., 1988, Calibration and application of Marinelli beakers. UCRL-53779, LLNL, p. 32-34.

Federal Register, 1991, 58, 33120-33121.

Fritz, P., Fontes, J. Ch., 1986, Handbook of Environmental Isotope Geochemistry. Vols. 1-2. Elsevier: New York, 557 pgs.

Frölich, K., et al., 1991, Application of isotopic methods to dating of very old groundwaters: Milk River aquifer, Alberta, Canada. Appl. Geochem., 6, 465-472.

Goldberg, E.D., Minoru, K., Schmitt, R.A., Smith, R.H., 1963, Rare-earth distributions in the marine environment. Jour. Geophy. Res., 68, p. 4209-4217.

Grove, D.B., Rubin, M., Hanshaw, B.B., Beetem, W.A., 1969, Carbon-14 dates of groundwater from a Paleozoic carbonate aquifer, south-central Nevada. U.S. Geol. Survey Prof. Paper 650-C, p. C215-C218.

Gunnink, R. and Niday, J.B., 1972, Computerized quantitative analysis by gamma-ray spectrometry. UCRL-51061, LLNL.

Hendry, M.J. and Schwartz, F.W., 1988, An alternative view on the origin of chemical and isotopic patterns in groundwater from the Milk River aquifer, Canada. Water Resour. Res., 24, p. 1747-1763.

Horwitz, E.P., Dietz, M.L., Fisher, D.E., 1991, Separation and preconcentration of strontium from biological, environmental, and nuclear waste samples by extraction chromatography using a crown ether. Anal. Chem., 63, 522-525.

Knauss, K.G., 1984, Petrologic and geochemical characterization of the Tonopah Spring Member of the Paintbrush Tuff: Outcrop samples used in waste packaging experiments. Lawrence Livermore Lab UCRL-53558, 36 pgs.

Lyles, B.F. and Mihevc, T.M., 1992, NTS groundwater recharge study, FY 1992. Desert Research Institute. 40 pgs.

Marshall, B.D., Z.E. Peterman and J.S. Stuckless, 1993, Strontium isotopic evidence for a higher water table at Yucca Mountain, High Level Radioactive Waste Management, Proceedings of Fourth International Conference, American Nuclear Society and American Society of Civil Engineers, p. 1948 -1952.

Mazor, E., 1991, Applied Chemical and Isotopic Groundwater Hydrology. Halsted Press: New York, 274 pgs.

Mazor, E., 1972, Paleotemperatures and other hydrological parameters deduced from noble gases dissolved in groundwater; Jordan Rift Valley, Israel. Geochim. Cosmochim. Acta, 36, p. 1321-1336.

Mifflin, M.D. and Hess, J.W., 1979, Regional carbonate flow systems in Nevada. J. Hydrol., 43, 217-237.

Nolte, E., Krauthan, P., Korschinek, G., Maloszewski, P., Fritz, P., Wolf, M., 1991, Measurements and interpretations of ^{36}Cl in groundwater, Milk River aquifer, Albert, Canada. Applied Geochem., 6, 435-445.

Nordstrom, D.K., Olsson, T., Carlsson, L., Fritz, P., 1989, Introduction to the hydrogeochemical investigations within the International Stripa Project. Geochim. Cosmochim. Acta, 53, 1717-1726.

Norris, A.E., Wolfsberg, K., Gifford, S.K., Bentley, H.W., Elmore, D., 1987, Infiltration at Yucca Mountain, Nevada, traced by ^{36}Cl. Nuclear Instr. Methods. Phys. Res., B29, p. 376-379.

O'Nions, R. K. and Oxburgh, E.R., 1983, Heat and helium in the earth: Nature, 306, p. 429-431.

Osmond, J.K. and Cowart, J.B., Groundwater. in Ivanovich, M. and Harmon, R.S., eds. Uranium Series Disequilibrium: Applications to Environmental Problems. Clarendon Press: Oxford. p. 202-245.

Pearson, F.J. Jr., et al., 1991, Applied Isotope Hydrology, A Case Study in Northern Switzerland. Studies in Environmental Science 43, Elservier: New York.

Peterman, Z.E., J.S. Stuckless, B.D. Marshall, S.A. Mahan and K. Futa, 1992a, Strontium isotope geochemistry of calcite fracture fillings in deep core, Yucca Mountain,

Nevada - a progress report, High Level Radioactive Waste Management, Proceedings of the Third International Conference, American Nuclear Society and American Society of Civil Engineers, p. 1582 - 1586.

Peterman, Z.E., Stuckless, J.S., Mahan, S.A., Marshall, B.D., Gutentag, E.D., Downey, J.S., 1992b, Strontium isotope characterization of the Ash Meadows groundwater system, southern Nevada, USA. in Kharaka, Y.K., Maest, A.S., eds. Proceedings of the 7th International Symposium on Water-Rock Interaction-WRI-7, Park City, Utah, p. 825-829.

Phillips, F.M., Bentley, H.W., Davis, S.N., Elmore, D., Swanick, G.B., 1986, Chlorine-36 dating of very old groundwater: 2. Milk River aquifer, Alberta, Canada. Water Resour. Res., 22, p. 2003-2016.

Phillips, F.M., Mattick, J.L., Duval, T.A., Elmore, D., Kubik, P.W., 1988, Chlorine-36 and tritium from nuclear weapons fallout as tracers for long-term liquid and vapor movement in deserts soils. Water Resour. Res., 24, p. 1877-1891.

Raytheon Services Nevada (1990) Nevada Test Site drilling and mining summary. "The Red Book".

Ruggieri, M.R., Tyler, S., Buddemeier, R.W., 1988, Infiltration and recharge (Cambric event site), in Buddemeier, R.W., ed., Hydrology and Radionuclide Migration Program 1985-1986 Progress Report. Lawrence Livermore Lab. UCRL-53779, 47 pgs.

Schoff, S.L. and Moore, J.E., 1964, Chemistry and movement of groundwater, Nevada Test Site. USGS Trace Element Investigations TEI-838, 75 pgs.

Silva, R.J., Evans, R., Rego, J.H., Buddemeier, R.W., 1986, Technetium analyses in the radionuclide migration project. Nuclear Chemistry Division FY86 Annual Report, LLNL, p. 14-16.

Smith, D.K., 1993, A review of literature pertaining to the leaching and sorption of radionuclides associated with nuclear explosive melt glasses. Lawrence Livermore Lab., UCRL-ID-113370, 26 pgs.

Spencer, E.B., 1990, A radiocarbon study of groundwater in the western Nevada Test Site and vicinity. Master's Thesis, University of Nevada, Reno. 124 pgs.

Stuckless, J.S., Peterman, Z.E., Muhs, D.R., 1991, U and Sr isotopes in groundwater and calcite, Yucca Mountain, Nevada: Evidence against upwelling water. Science, 254, p. 551-554.

Stuiver, M. and Polach, H.A., 1977, Reporting of ^{14}C data. Radiocarbon, 19, p. 355-363.

Surano, K.A., Hudson, G.B., Failor, R.A., Sims, J.M., Holland, R.C., MacLean, S.C., Garrison, J.C., 1992, Helium-3 mass spectrometry for low -level tritium analysis of environmental samples. Jour. Radioanal. Nuclear Chem. Art., 161, p. 443-453.

Thompson, P.H., 1991, Geothermal investigation of LANL areas of Yucca Flat. Letter to K. Hahn at LANL. Raytheon Services Nevada-Geology/Hydrology Division. 11 pgs.

Torgerson, T. and Clarke, W. B., 1985, Helium accumulation in groundwater, I: An evaluation of the sources and the continental flux of crustal ^{4}He in the Great Artesian Basin, Australia. Geochimica st Cosmochimica Acta, 49, p. 1211-1218.

Weiss, W. and Roether, W., 1980, The rates of tritium input to the world oceans. Earth Planet. Sci. Lett., 49, 435-446.

Winograd, I.J., Thordarson, W., 1975, Hydrogeologic and hydrochemical framework, south-central Great Basin, Nevada-California, with special reference to the Nevada Test Site. U.S. Geological Survey Professional Paper 712-C. 126 pgs.

Winograd, I.J. and Pearson, F.J., 1976, Major carbon 14 anomaly in a regional carbonate aquifer: possible evidence for megascale channeling, south central Great Basin. Water Resources Research, 12, 1125-1143.

Winograd, I.J. and Robertson, F.N., 1982, Deep oxygenated groundwater: anomaly or common occurrence? Science, 216, 1227-1229.

FIGURE CAPTIONS

Figure 1. Location map after Winograd and Thordarson (1975) showing the Nevada Test Site. Highlighted groundwater level contours suggest groundwater flow directions. Downward flow is inferred in Yucca and Frenchman Flats where contours are enclosed. Note also that groundwater elevations are ~600 meters higher on Pahute Mesa.

Figure 2. General sketch of equipment used at the well head for open hole sampling.

Figure 3. Locations of all the wells sampled during FY 92-93. Note that most of the wells generally lie in a northwest-southeast direction from Pahute Mesa to Frenchman Flat.

Figure 4. Water level elevations have a bimodal distribution separating wells located at higher elevations from wells located at lower elevations. The horizontal distribution of the water levels relative to the penetration depth suggests normal hydrostatic pressures, where deviations from horizontal may indicate non-hydrostatic pressures.

Figure 5. The water levels in the NTS wells do not form a unit regression, where rates of increase in surface elevation commonly are higher than rates of increase in water elevations.

Figure 6. Mapped are the down-hole temperature measurements collected during the FY 92-93 field seasons. Although some of the temperature variation is attributable to differences in the sample depth, abnormal temperature gradients exist below the surface at Pahute Mesa and eastern Yucca Flat.

Figure 7. Cross-section running northwest-southeast through Yucca Flat with measured temperatures contoured. Note the high horizontal temperature gradient (0.33°F/100ft) between wells ER-6-1 and TW-B.

Figure 8. Na and K most likely are derived from the volcanic tuffs, while Ca and Mg are predominantly from the Paleozoic carbonates. The one-to-one relationship suggests that no additional sources may be independently controlling these concentrations in the groundwater.

Figure 9. Piper plot showing a distinct mixing line between a Na-HCO_3 end-member and a mixed Ca-Mg-Na-HCO_3 groundwater at the test site. Similar diagrams have been presented by Winograd and Thordarson (1975) and Chapman and Lyles (1993).

Figure 10. The ^{14}C decrease in the NTS groundwaters correlates with $\delta^{13}C$ enrichment indicating the influence of "dead" dissolved carbonate. Some of the enrichment of $\delta^{13}C$ may be from isotopic equilibration between the Paleozoic carbonates and the dissolved bicarbonate in the groundwater that occur, in part, independent of increased dissolution of the Paleozoic carbonates.

Figure 11. Possible mechanisms that increase the uncertainty in the ^{14}C calculated ages from groundwater at the NTS.

Figure 12. The $^{36}Cl/Cl$ ratios of the NTS groundwaters are compared to those from the Dakota Aquifer of Kansas. Both groundwaters show a common trend of "dead" Cl enrichment that is matched by a decrease in the $^{36}Cl/Cl$ ratios. Possible sources of "dead" Cl at the NTS may include the Paleozoic carbonates and volcanic tuffs, or small amounts of residual marine waters still in the marine sediments.

Figure 13. Increased Si concentrations appear to be related to groundwater residing in volcanic tuffs at the NTS, whereas Ca enrichments are probably related to Paleozoic carbonates. The $^{87}Sr/^{86}Sr$ values in this figure suggests that a more radiogenic groundwater source is indicative of the higher Ca waters derived from the Paleozoic carbonates.

Figure 14. More radiogenic $^{87}Sr/^{86}Sr$ signatures tend to be related to higher bicarbonate concentrations in the groundwater, where the positive trend is most likely related to increases in dissolution of the Paleozoic carbonates.

Figure 15. The ^{234}U-excess (where the ^{234}U excess = (activity ratio - 1)[U]) for southwestern Nevada groundwater is compared to their uranium concentrations (after Osmond and Cowart, 1982). Osmond and Cowart (1982) suggested that the oxidized waters in this region allow conservative treatment of the uranium mobility in the groundwater. They suggested that the data in this figure represents mixing of different water masses in the hypothesized regional flow system for the region. Well UE-1q is from Yucca Flat (considered separate from the regional flow) and has a higher ^{234}U-excess than those within the mixing diagram. HS=Hi Ko Spr., CS=Crystal Spr., PWS=Pederson Warm Spr., AS=Ash Spr., DH=Devil's Hole, AT=Armagosa Test Well, KS=King Spr., CP=Crystal Pool, BS=Big Spr., RS=Rogers Spr., FBSW=Fairbanks Spr. southwest, FBNE=Fairbanmks Spr. northeast, IS=Indian Spr., ARMY=Army Well #1, CC=Cold Spr., TS=Trout Spr., TrS=Travertine Spr., TxS=Texas Spr., NS=Nevares Spr., WJF=Jackass Flats welded tuff aquifer, WFF=Frenchman Flats welded tuff aquifer, AFF=Frenchman Flats alluvial aquifer, YF=Yucca Flats, Paleozoic carbonate aquifer.


NEVADA TEST SITE
NEVADA TEST SITE
Approximate boundary
N
0
8
16 km

Figure 1.

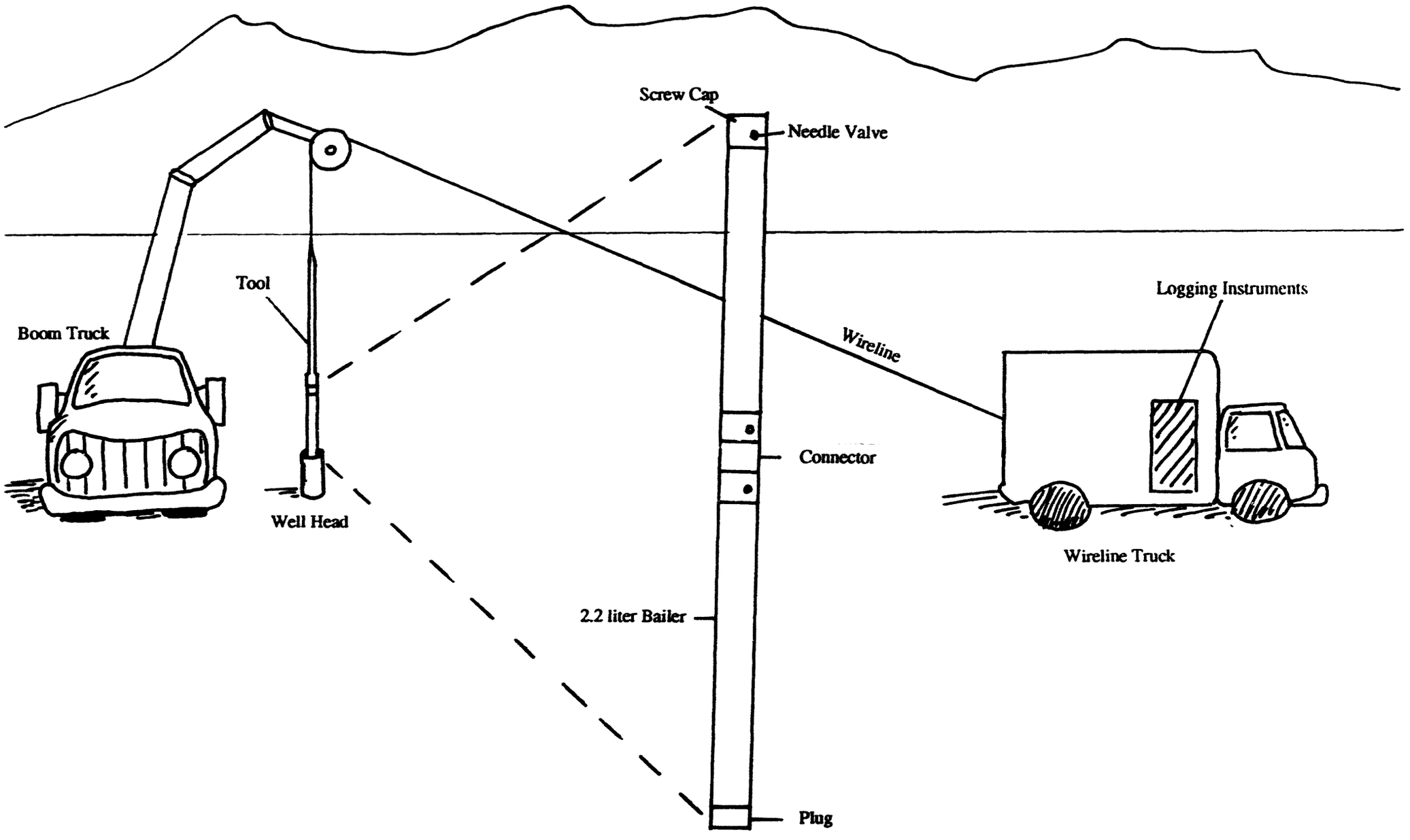
Screw Cap
Needle Valve
Tool
Boom Truck
Wireline
Logging Instruments
Connector
Well Head
Wireline Truck
2.2 liter Bailer
Plug

Figure 2.

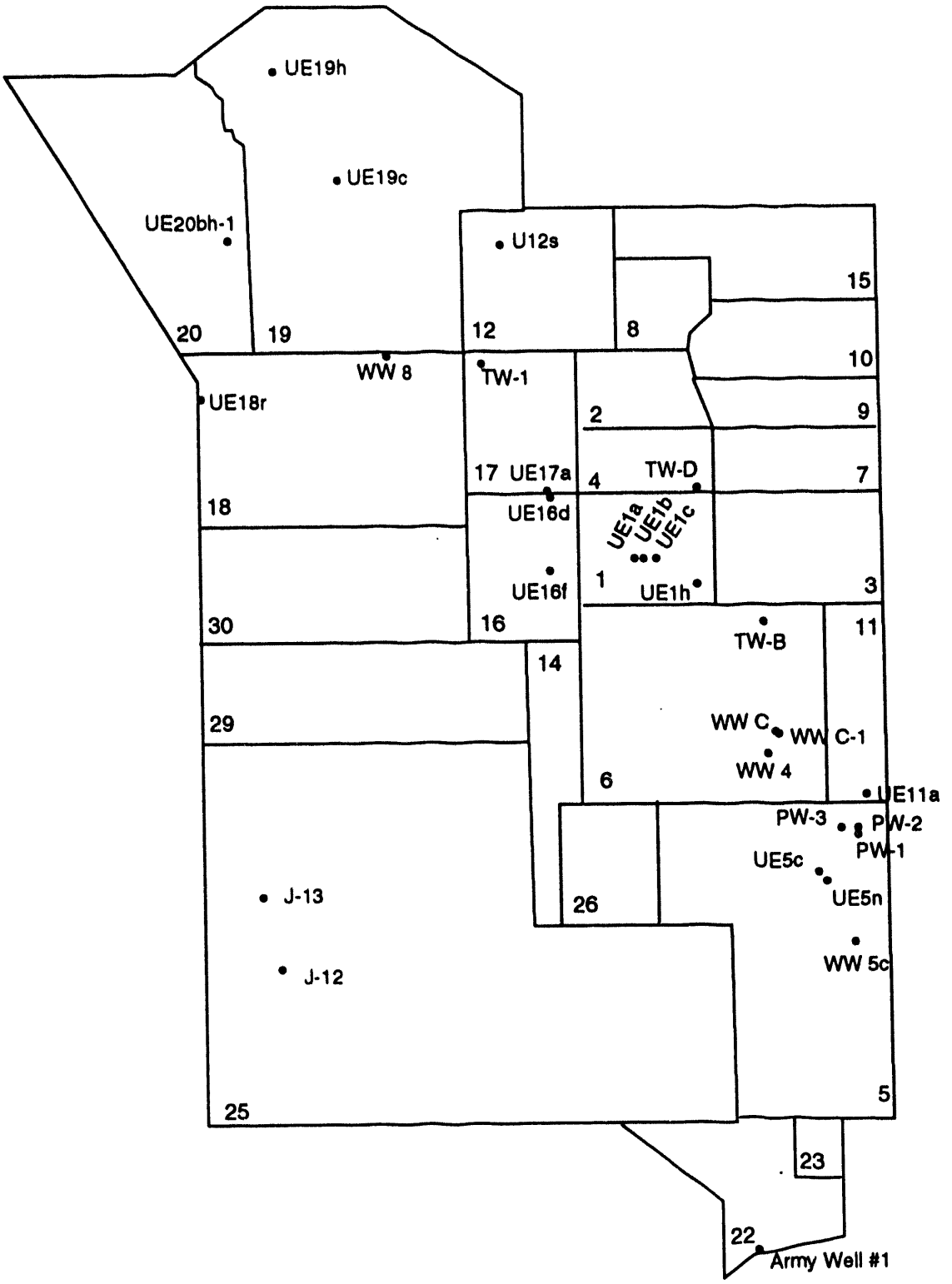
UE19h
UE19c
UE20bh-1
U12s
15
20
19
12
8
10
WW 8
TW-1
UE18r
2
9
17
UE17a
4
TW-D
7
18
UE16d
UE1a
UE1b
UE1c
1
UE1h
3
UE16f
30
16
TW-B
11
14
29
WW C
WW C-1
WW 4
6
UE11a
PW-3
PW-2
PW-1
UE5c
J-13
26
UE5n
WW 5c
J-12
5
25
23
22
Army Well #1

Figure 3

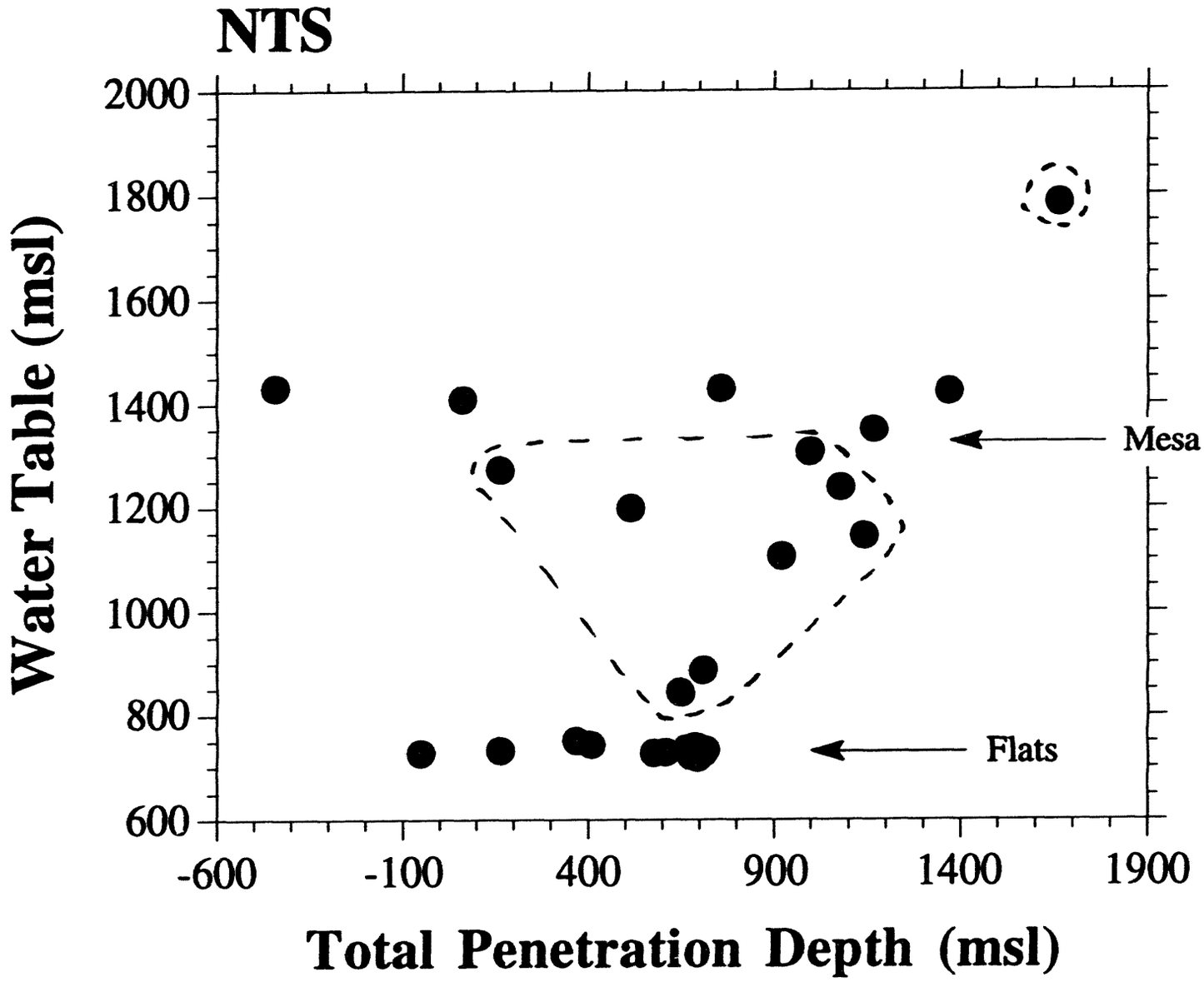
NTS
Water Table (msl)
2000
1800
1600
1400
1200
1000
800
600
-600
-100
400
900
1400
1900
Total Penetration Depth (msl)
Mesa
Flats

Figure 4.

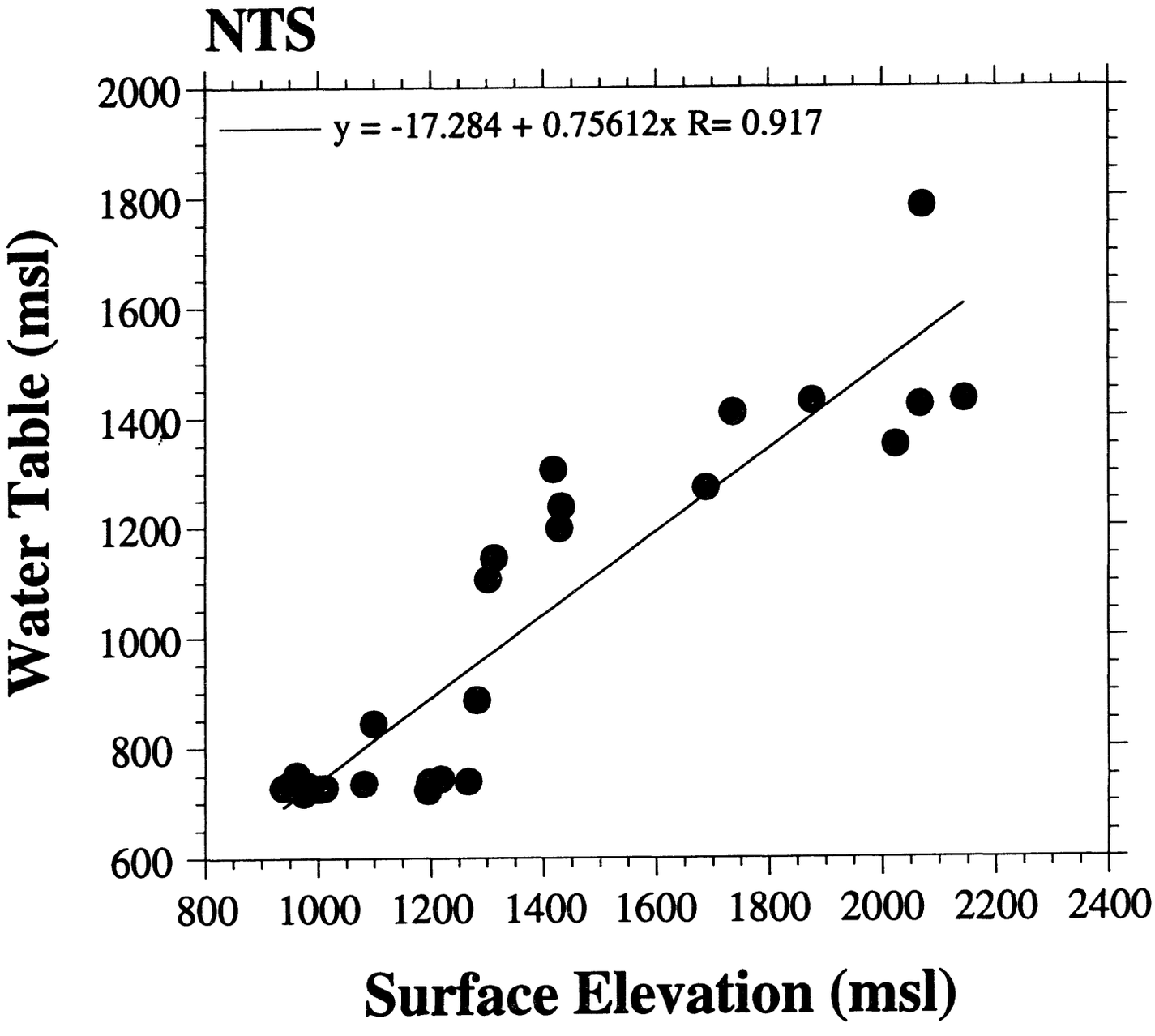
NTS
y = -17.284 + 0.75612x R= 0.917
Water Table (msl)
Surface Elevation (msl)
2000
1800
1600
1400
1200
1000
800
600
800
1000
1200
1400
1600
1800
2000
2200
2400

Figure 5.

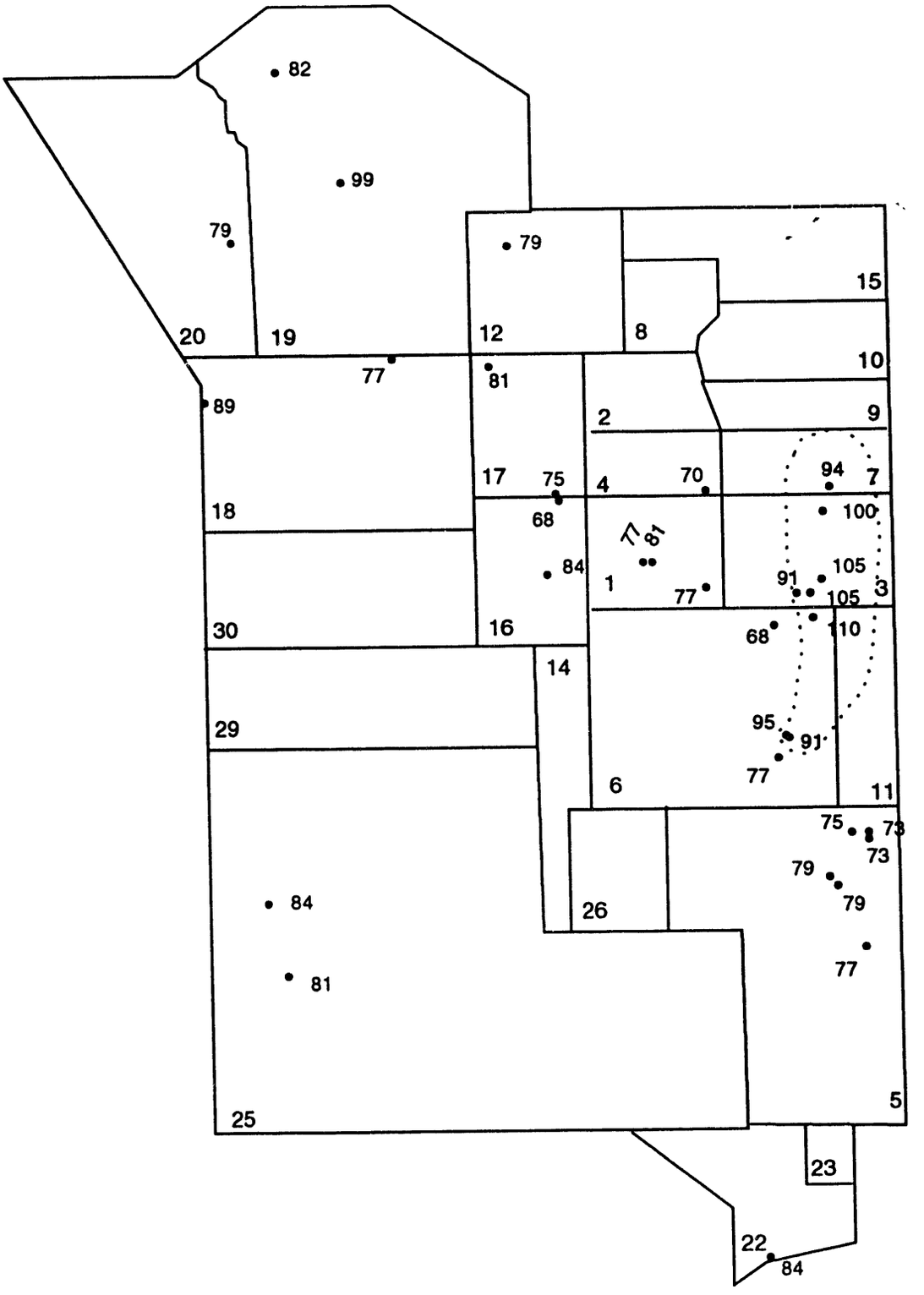
82
99
79
79
15
20
19
12
8
10
77
81
89
2
9
17
75
4
70
94
7
18
68
100
84
1
77
91
105
105
3
30
16
68
110
14
29
95
91
77
6
11
75
73
73
79
84
26
79
81
77
5
25
23
22
84

Figure 6

Temperature cross section from Syncline Ridge to Frenchman Flat

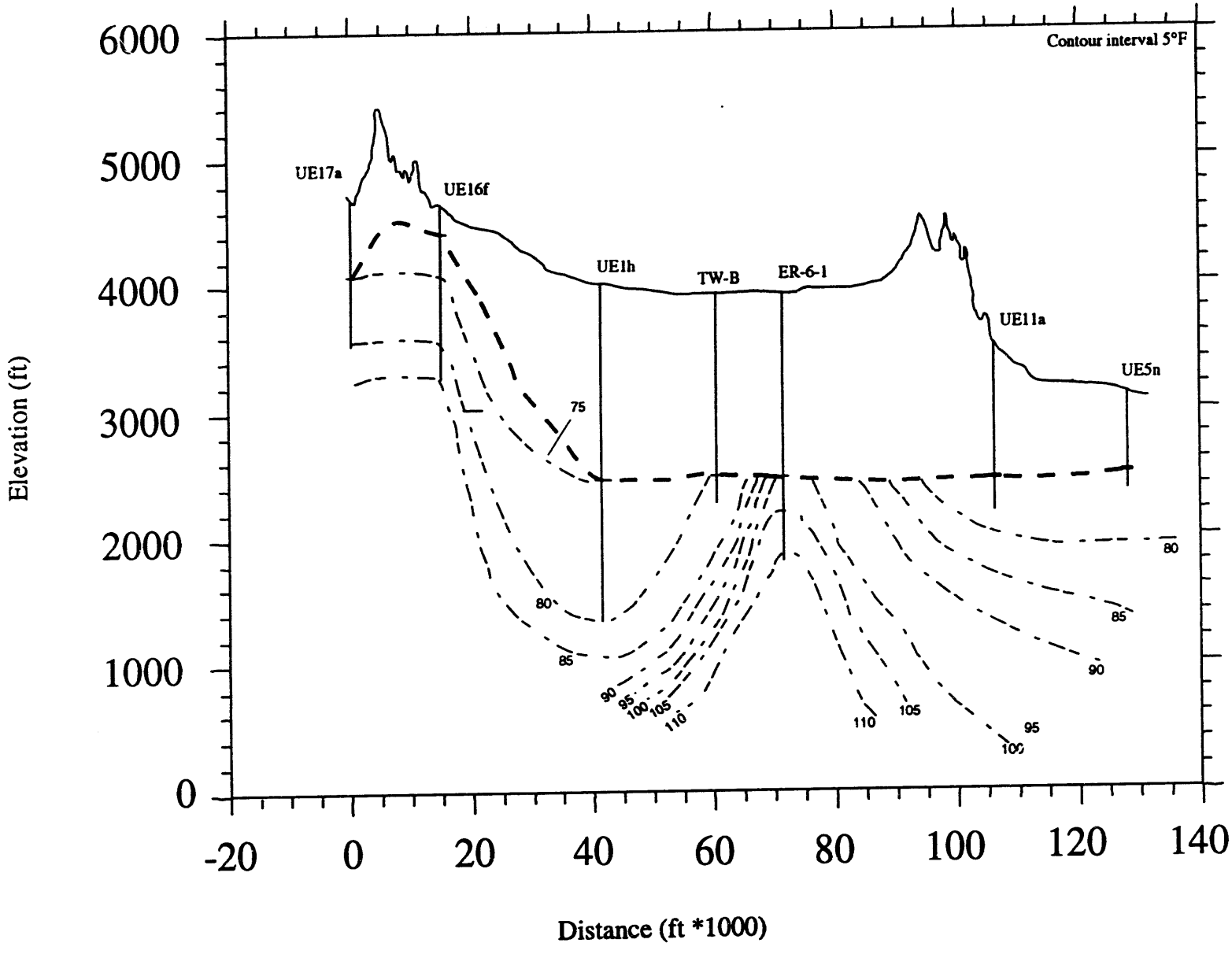

Figure 7

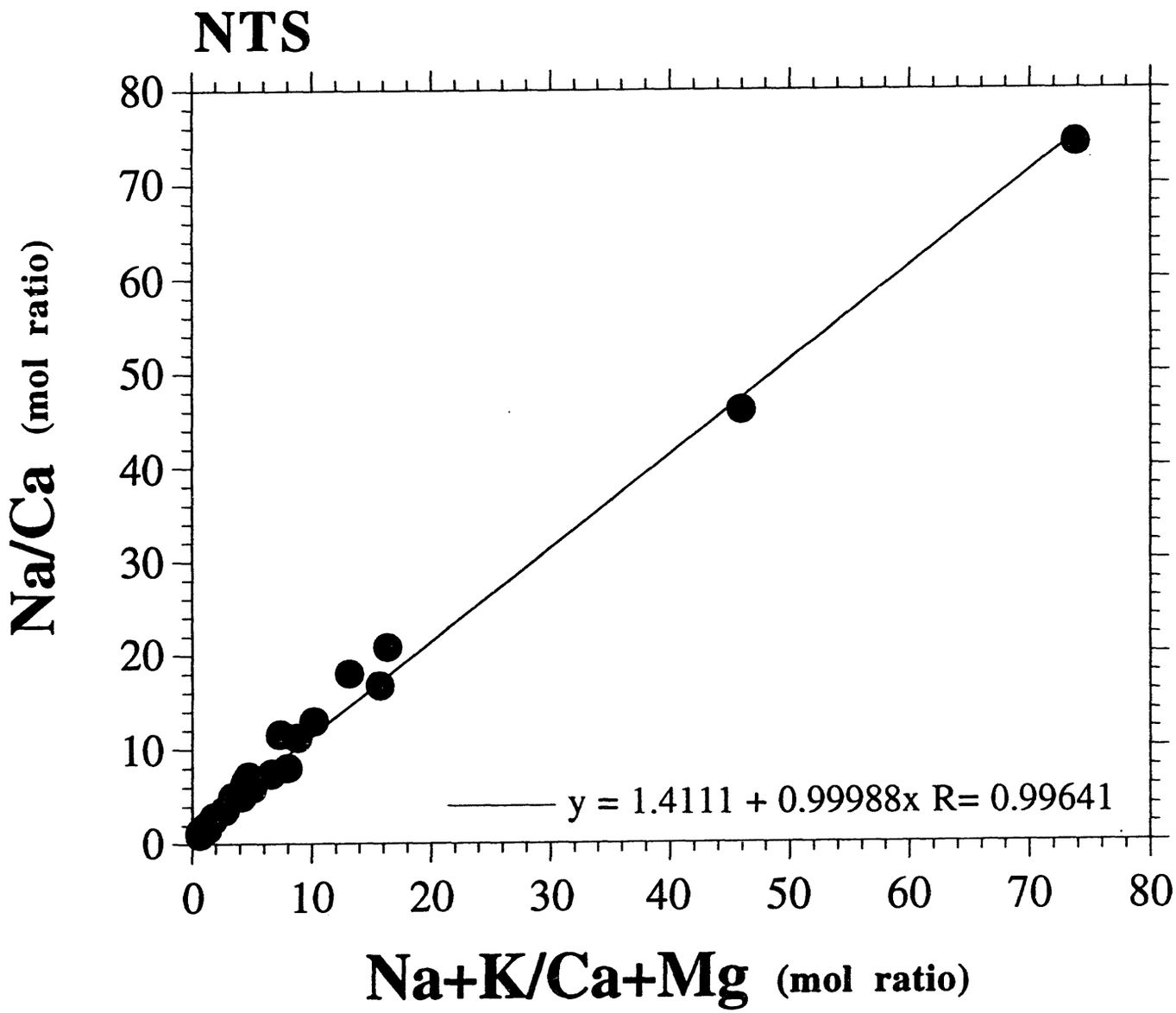
NTS
Na/Ca (mol ratio)
Na+K/Ca+Mg (mol ratio)
y = 1.4111 + 0.99988x R= 0.99641
0
10
20
30
40
50
60
70
80

Figure 8.

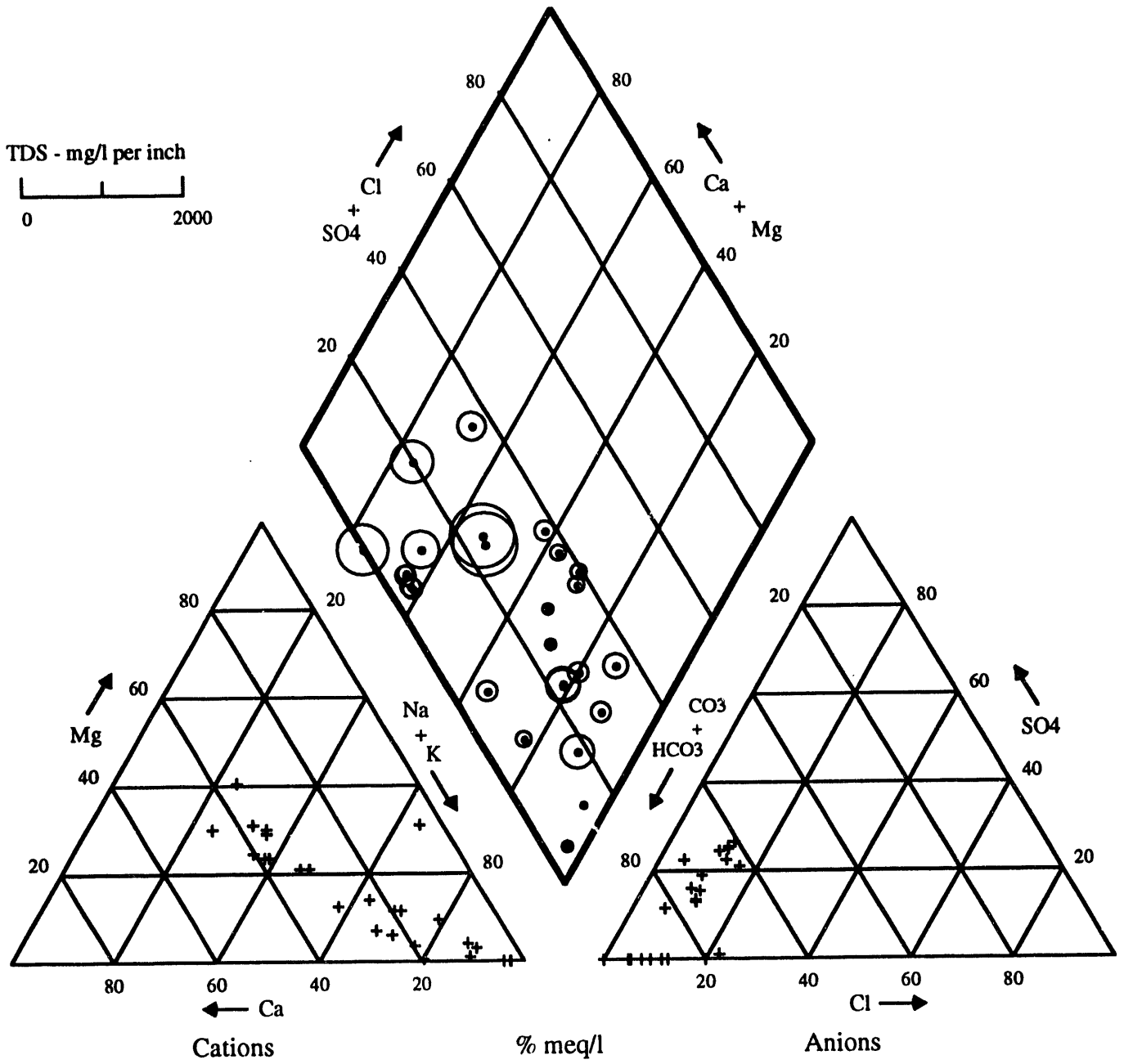
TDS - mg/l per inch
0
2000
Cl
+
SO4
Ca
+
Mg
Mg
Na
+
K
CO3
+
HCO3
SO4
Ca
Cl
80
60
40
20
Cations
% meq/l
Anions

Figure 9

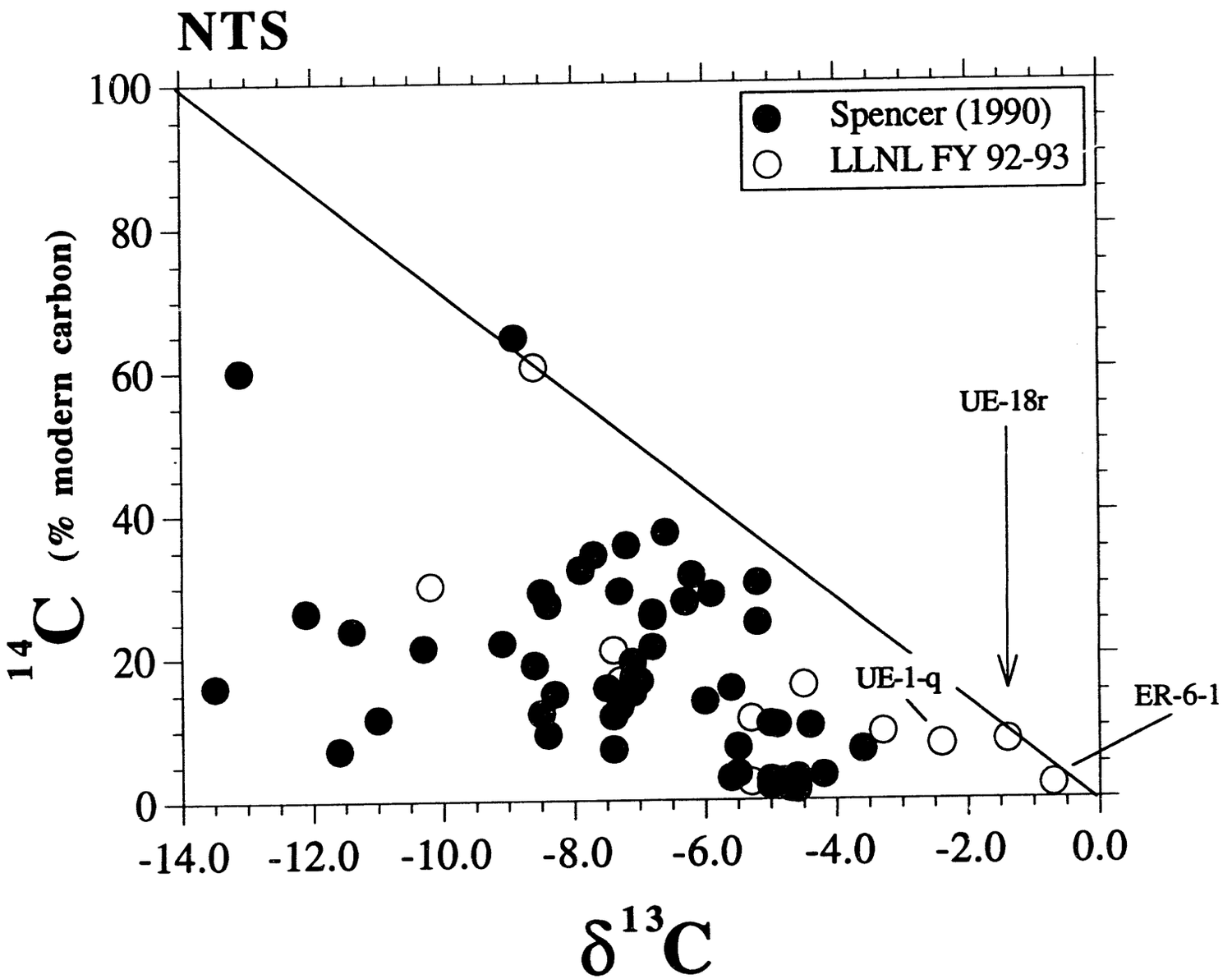
NTS
Spencer (1990)
LLNL FY 92-93
UE-18r
UE-1-q
ER-6-1
100
80
60
40
20
0
-14.0
-12.0
-10.0
-8.0
-6.0
-4.0
-2.0
0.0
^{14}C (% modern carbon)
$\delta^{13}C$

Figure 10.

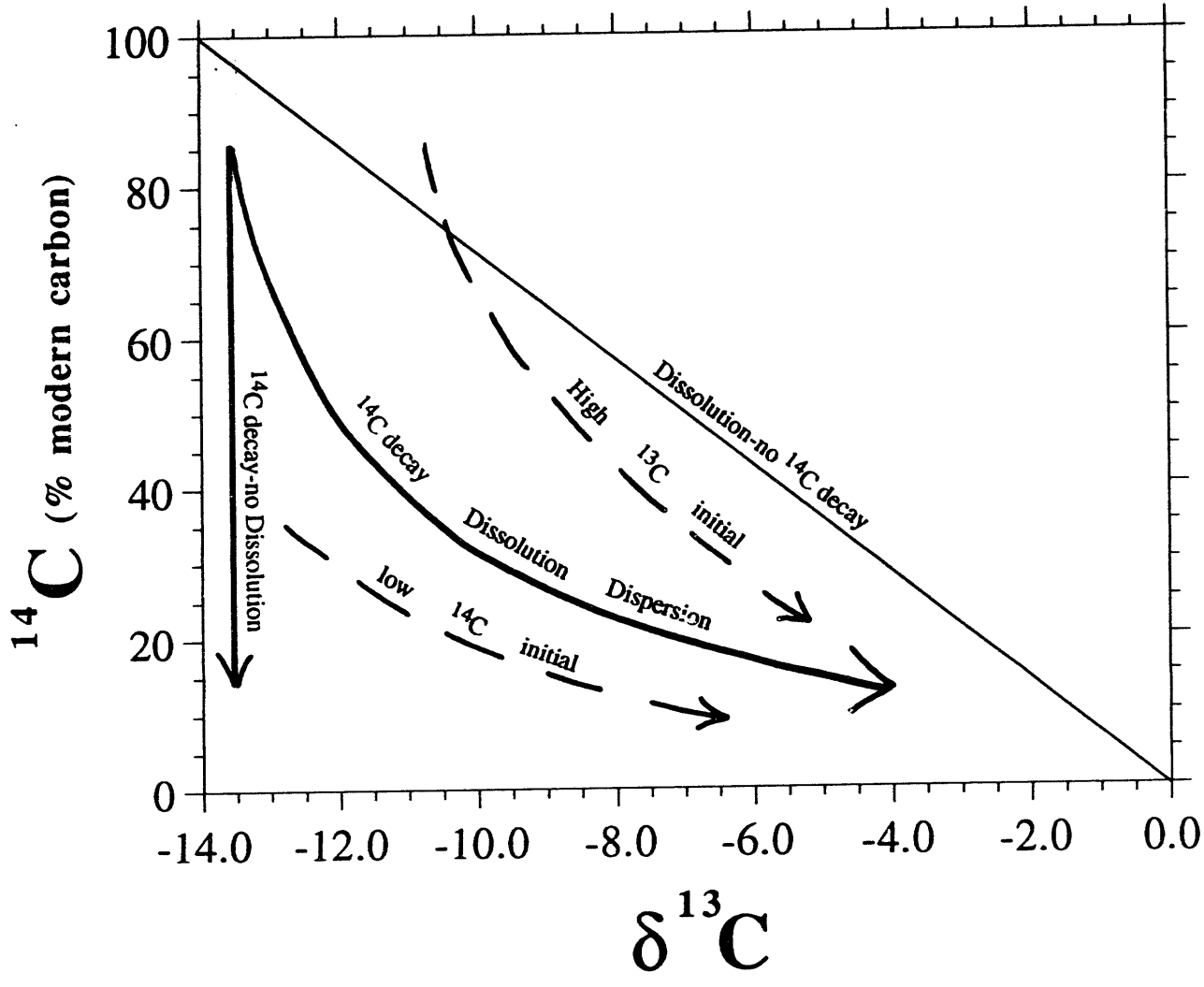
100
80
60
40
20
0
-14.0
-12.0
-10.0
-8.0
-6.0
-4.0
-2.0
0.0
^{14}C (% modern carbon)
$\delta^{13}C$
^{14}C decay-no Dissolution
^{14}C decay
Dissolution
Dispersion
Dissolution-no ^{14}C decay
High ^{13}C initial
low ^{14}C initial

Figure 11.

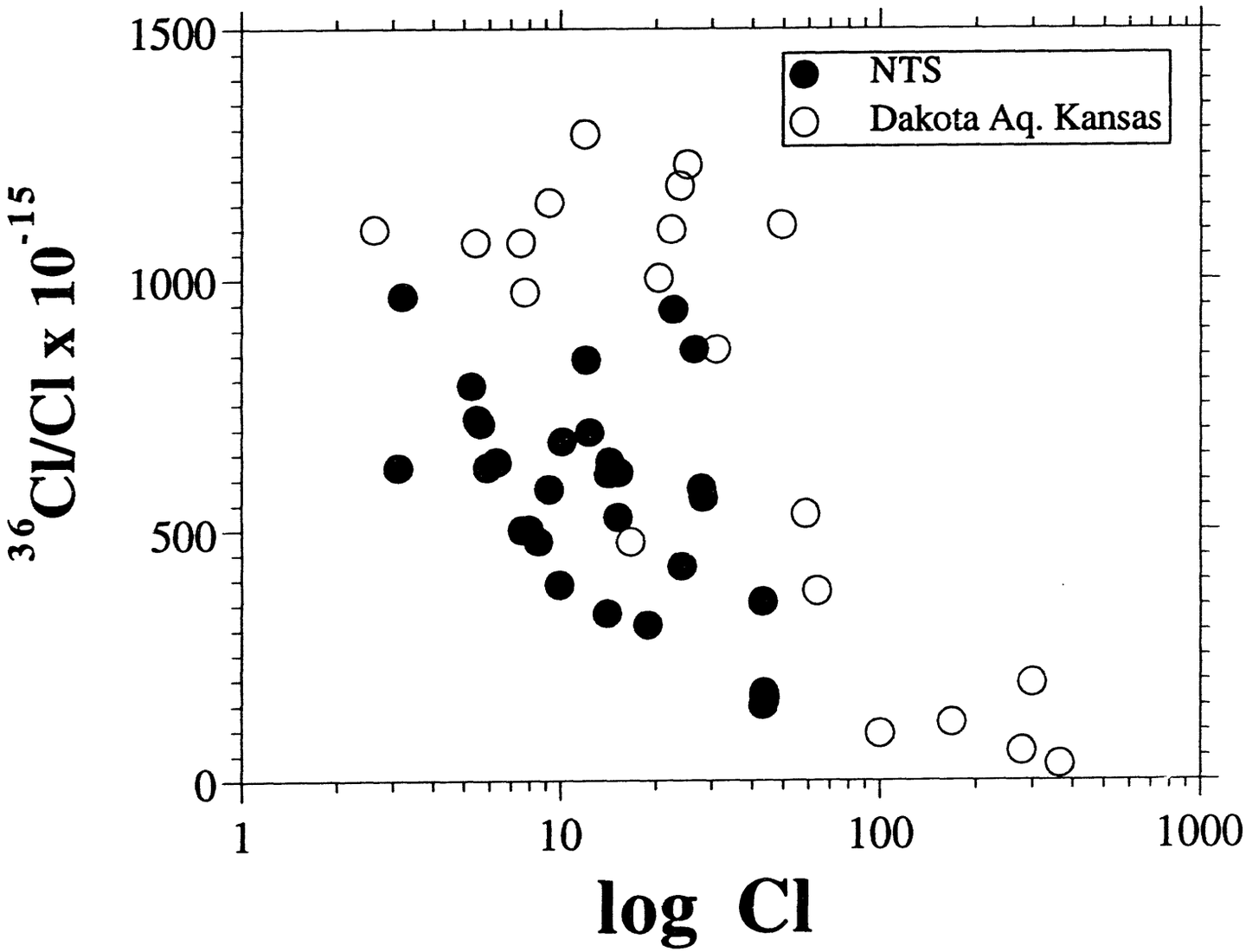
1500
1000
500
0
1
10
100
1000
log Cl
^{36}Cl/Cl x 10^{-15}
NTS
Dakota Aq. Kansas

Figure 12.

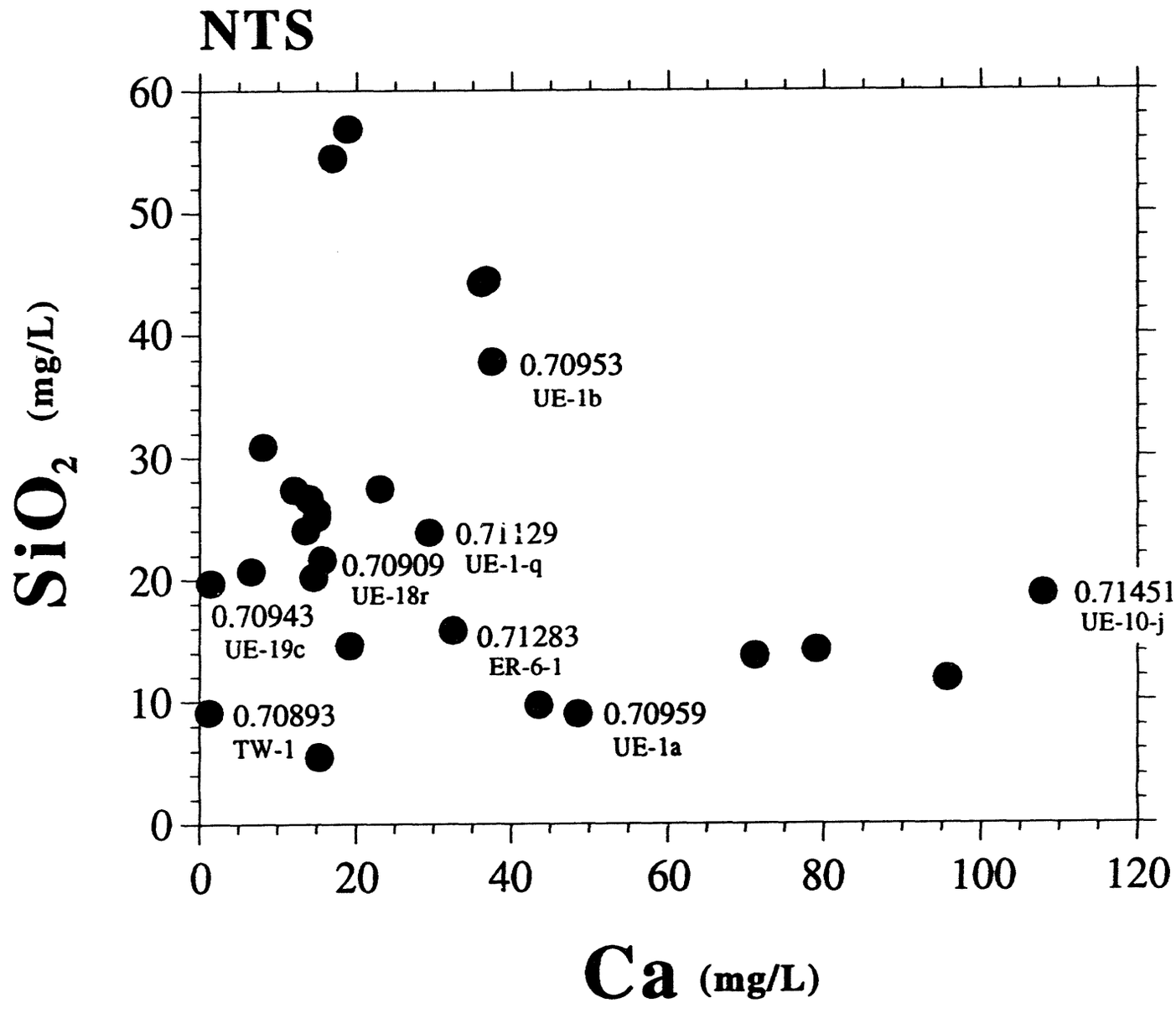
NTS
60
50
40
30
20
10
0
0
20
40
60
80
100
120
SiO2 (mg/L)
Ca (mg/L)
0.70953
UE-1b
0.71129
UE-1-q
0.70909
UE-18r
0.70943
UE-19c
0.71283
ER-6-1
0.71451
UE-10-j
0.70893
TW-1
0.70959
UE-1a

Figure 13.

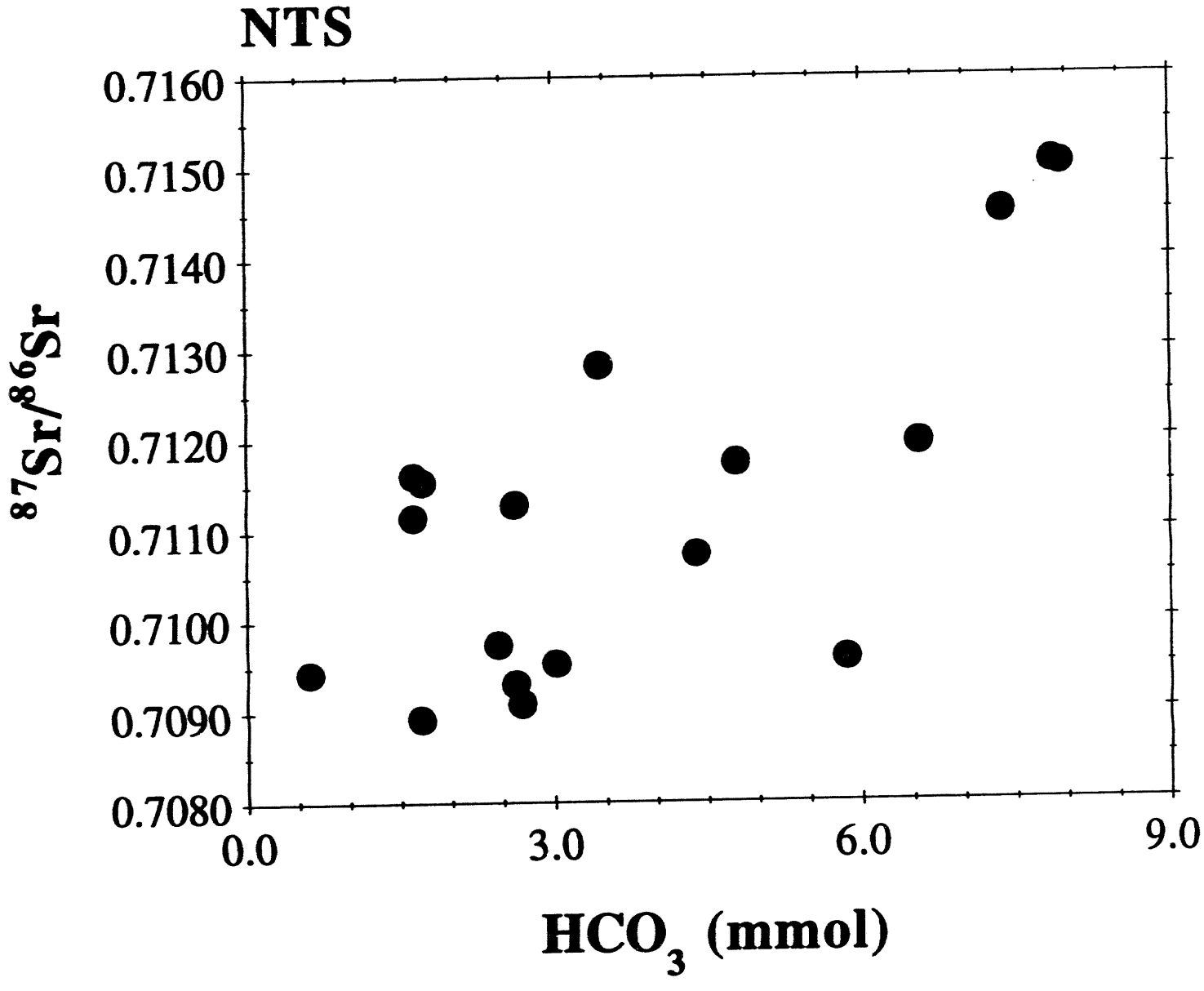
NTS
0.7160
0.7150
0.7140
0.7130
0.7120
0.7110
0.7100
0.7090
0.7080
$^{87}Sr/^{86}Sr$
0.0
3.0
6.0
9.0
HCO_3 (mmol)

Figure 14.

(From Osmond and Cowart, 1982)

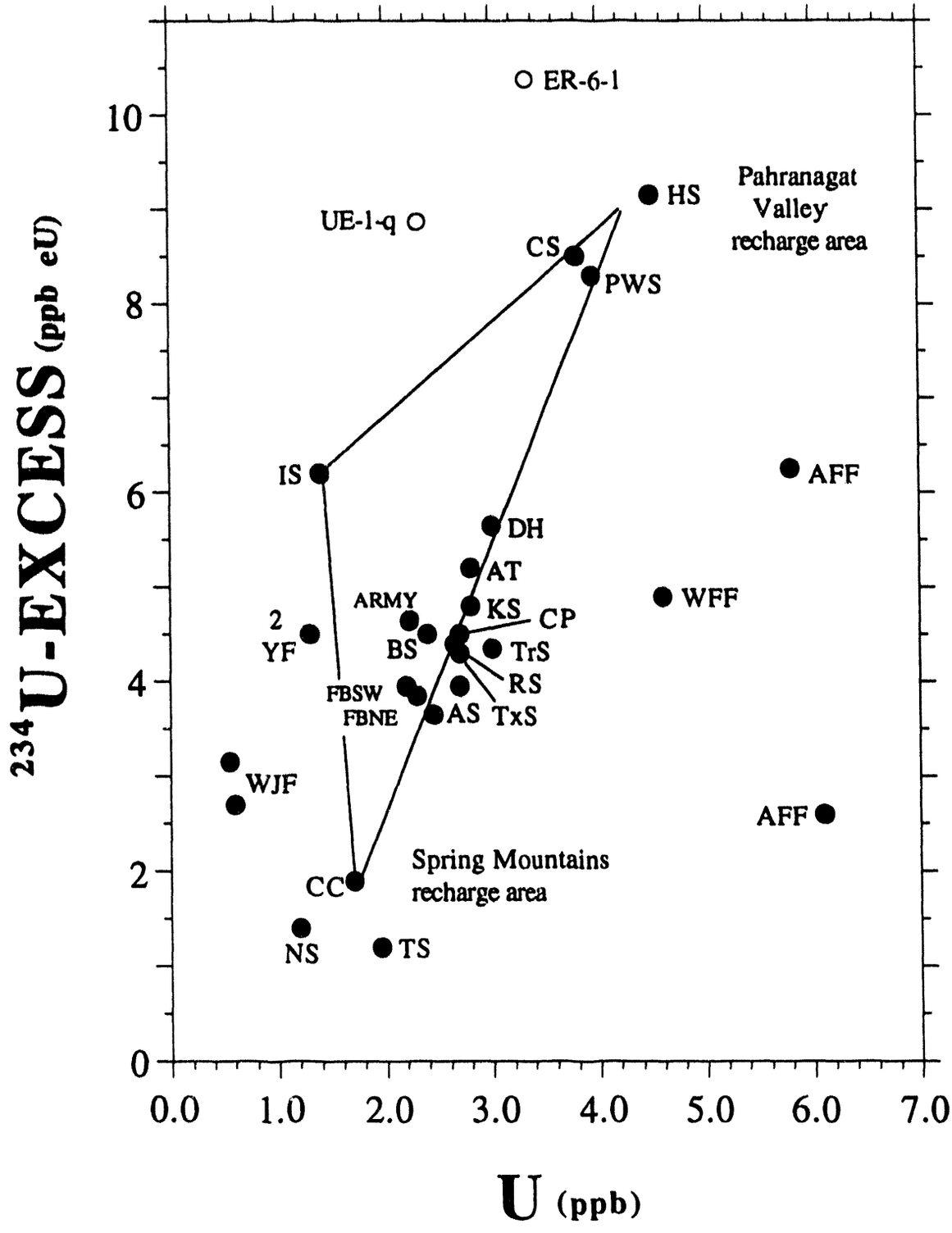

Figure 15.

Table 1: HRMP FY 92-93

Wells	Sample Date	NTS Area	Total Depth (msl)	Depths sampled (msl)
UE-1a*	9/1/92	1	1141	1144
UE-1b*	9/1/92	1	920	1095
UE-1c*	9/2/92	1	709	870, 783
UE-1h	5/26/93	1	407	614, 566
TW-D	6/8/93	4	687	717
UE-5n	5/24/93	5	715	728
PW-1*^	5/26/93	5	714	718
PW-2*^	5/25/93	5	695	703
PW-3*^	5/26/93	5	709	712
TW-B	6/7/93	6	693	710
UE-11a	5/25/93	11	667	NONE
U-12s	7/13/93	12	1664	1675
UE-16f	7/12/93	16	996	1023
TW-1*	8/13/92	17	756	1252
UE-17a	6/9/93	17	1078	1178, 1129, 1101
UE-18r*	8/11/92	18	163	1179
UE-19h*	8/12/92	19	1368	1399
UE-20bh-1*	6/20/93	20	1167	1173
Water Supply Wells				
UE-5c*	5/13/93	5	163	639
WW- 5c*	5/20/93	5	577	625
WW-C*	5/19/93	6	677	722
WW-C1*	5/19/93	6	675	710
WW-4*	5/20/93	6	647	683
UE-16d*	6/2/93	16	513	1093
WW-8*	6/2/93	18	62	1359
UE-19c*	8/13/92	19	-444	1372
Army Well #1*	5/12/93	22	368	613
J-13*	5/13/93	25	-52	654
J-12*	5/13/93	25	607	700
GCP Wells				
UE-1q	7/10/92	1	452	495
ER-6-1	10/9/92	6	551	655

*Total depth from Raytheon Services Nevada "Nevada Test Site Drilling and Mining Summary".

^Well elevations approximated from USGS 15' topographical sheets.

Numbers in parenthesis are msl elevations of the bottom of linings.

All elevations are in meters relative to sealevel

Table 1: HRMP FY 92-93

Wells	Surface Elev (msl)	Water Table (msl)	Casing Depth (msl)
UE-1a*	1312	1145	1288
UE-1b*	1302	1106	1279
UE-1c*	1282	887	1259
UE-1h	1218	744	567
TW-D	1266	740	747
UE-5n	949	734	484 (686)
PW-1*^	969	733	719
PW-2*^	975	718	704
PW-3*^	1000	727	714
TW-B	1198	739	728 (687)
UE-11a	1081	736	899
U-12s	2071	1784	2067
UE-16f	1418	1306	1024
TW-1*	1876	1430	1384 (745)
UE-17a	1432	1238	1063
UE-18r*	1688	1272	1192
UE-19h*	2067	1423	1372
UE-20bh-1*	2023	1350	1433
Water Supply Wells			
UE-5c*	980	733	980
WW- 5c*	939	728	577
WW-C*	1195	725	777 (700)
WW-C1*	1195	723	918 (692)
WW-4*	1098	844	660
UE-16d*	1428	1198	782
WW-8*	1736	1409	1736 (838)
UE-19c*	2144	1432	1406
Army Well #1*	961	751	576 (547)
J-13*	1011	728	540 (-20)
J-12*	954	729	684
GCP Wells			
UE-1q	1244	-	495
ER-6-1	1200	-	655

*Total depth from Raytheon Services Nevada "Nevada Test Site Drilling and Mining Summary".

^Well elevations approximated from USGS 15' topographical sheets.

Numbers in parenthesis are msl elevations of the bottom of linings.

All elevations are in meters relative to sealevel

Table 2: HRMP-FY 92-93

WELL	T°C	pH	TDS (mg/L)	Spec. Cond. (µS)	DO (mg/L)
UE-1a	25.4	7.35	348	692	3.0
UE-1b	27.4	7.41	217	448	4.0
UE-1c-1350	26.2	7.29	232	479	6.0
UE-1c-1636	36.2	7.45	226	452	5.0
UE-1h-1979	25.3	8.20	515	1029	-
UE-1h-2137	25.3	8.20	515	1029	-
U-3mi-1600	33.0	8.07	-	-	-
U-3mi-1650	33.0	8.07	-	-	-
TW-D	23.9	7.88	228	445	4.0
UE-5n	25.7	8.82	214	427	2.0
PW-1	22.5	8.67	407	407	3.0
PW-2	23.3	8.52	231	462	3.0
PW-3	24.1	9.30	198	295	3.0
TW-B	20.1	7.50	188	381	3.0
U-12s	26.1	10.45	-	632	7.0
UE-16f	29.4	8.85	-	1090	3.5
TW-1	26.6	8.66	118	238	2.0
UE-17a-831'	26.6	7.58	396	789	4.0
UE-17a-992'	23.9	7.63	400	803	1.5
UE-17a-1085'	24.4	8.27	1,090	1325	1.5
UE-18r	31.9	8.05	208	394	3.5
UE-19h	27.9	8.33	193	415	2.0
UE-20bh-1	25.8	8.26	93	186	12.0
Water Supply Wells					
UE-5c	26.3	8.01	227	452	5.5
WW-5c	25.4	8.81	302	603	3.0
WW-C	35.2	6.89	566	1135	3.0
WW-C1	32.7	6.54	563	1131	1.8
WW-4	25.3	7.39	207	415	6.0
UE-16d	20.4	-	360	717	<1.0
WW-8	25.0	-	97	194	6.0
UE-19c	36.5	7.71	87	174	6.0
Army Well #1	29.3	7.50	315	625	3.5
J-13	29.3	7.26	170	338	6.0
J-12	26.7	7.36	150	299	6.0
GCP Wells					
UE-1-q	31.2	7.80	-	-	-
ER-6-1	39.0	7.13	-	514	5.0
Post-Shot Wells					
UE-2ce	-	-	669	-	2.0
UE-3e#4-1630'	-	12.50	4,030	-	-
UE-3e#4-1785'	-	11.50	2,070	-	3.5
UE-3e#4-1885'	-	-	-	-	-
UE-3e#4-2150'	-	11.30	1,150	-	3.0
U-4t-PS-3A	-	7.55	377	-	3.0
U-4u-PS-2A	-	7.55	209	-	3.0
UE-7-ns	-	-	223	-	2.5

Table 2: HRMP-FY 92-93

WELL	Ca (mg/L)	Mg (mg/L)	Na (mg/L)	K (mg/L)	Na/Ca
UE-1a	48.5	23.9	50.5	8.7	1.0
UE-1b	37.4	13.7	31.3	10.7	0.8
UE-1c-1350	36.0	13.4	34.5	12.3	1.0
UE-1c-1636	36.7	13.7	33.7	12.4	0.9
UE-1h-1979	-	-	-	-	
UE-1h-2137	15.3	7.5	102.0	25.0	6.7
U-3mi-1600	16.9	3.3	126.3	7.1	7.5
U-3mi-1650	18.9	3.7	121.6	8.0	6.4
TW-D	-	-	-	-	
UE-5n	6.5	1.4	78.0	8.0	12.0
PW-1	14.9	5.4	57.0	6.0	3.8
PW-2	19.2	7.0	56.0	6.0	2.9
PW-3	14.5	5.6	60.0	7.0	4.1
TW-B	-	-	-	-	
U-12s	-	-	-	-	
UE-16f	-	-	-	-	
TW-1	1.2	-	51.3	0.5	42.8
UE-17a-331'	-	-	-	-	
UE-17a-992'	-	-	-	-	
UE-17a-1085'	-	-	-	-	
UE-18r	15.6	0.3	72.5	2.0	4.6
UE-19h	14.9	1.5	63.8	4.0	4.3
UE-20bh-1	-	-	-	-	
Water Supply Wells					
UE-5c	8.0	2.1	83.0	6.0	10.4
WW-5c	13.5	0.8	130.0	6.0	9.6
WW-C	71.1	29.6	118.0	13.0	1.7
WW-C1	79.0	30.2	119.0	13.0	1.5
WW-4	23.0	5.9	48.0	5.0	2.1
UE-16d	-	-	-	-	
WW-8	-	-	-	-	
UE-19c	1.4	-	35.8	0.5	25.6
Army Well #1	43.5	22.2	40.0	5.0	0.9
J-13	12.0	1.9	41.0	4.0	3.4
J-12	13.9	2.4	40.0	4.0	2.9
GCP Wells					
UE-1-q	29.4	15.3	31.2	4.6	1.1
ER-6-1	3.2	13.1	46.9	7.0	0.1
Post-Shot Wells					
UE-2ce	-	-	-	-	
UE-3e#4-1630'	-	-	-	-	
UE-3e#4-1785'	-	-	-	-	
UE-3e#4-1885'	-	-	-	-	
UE-3e#4-2150'	-	-	-	-	
U-4t-PS-3A	-	-	-	-	
U-4u-PS-2A	-	-	-	-	
UE-7-ns	-	-	-	-	

Table 2: HRMP-FY 92-93

WELL	Li (µg/L)	U (µg/L)	Sr (µg/L)	Mn (µg/L)	Fe (µg/L)	Si (mg/L)
UE-1a	-	-	630.0	100.0	1180.0	9.0
UE-1b	-	4.3	470.0	-	-	37.8
UE-1c-1350	-	4.1	410.0	-	-	44.3
UE-1c-1636	-	4.4	420.0	-	-	44.5
UE-1h-1979	-	-	169.0	41.3	-	-
UE-1h-2137	83.0	0.1	200.0	23.7	120.0	5.5
U-3mi-1600	80.0	18.5	480.0	50.0	120.0	54.5
U-3mi-1650	80.0	16.5	840.0	50.0	120.0	56.9
TW-D	-	-	-	-	-	-
UE-5n	21.0	2.6	46.0	15.6	170.0	20.7
PW-1	22.0	4.5	104.6	2.6	90.0	25.1
PW-2	23.0	6.3	186.0	41.1	100.0	14.6
PW-3	23.0	3.5	107.0	3.5	60.0	20.2
TW-B	-	0.8	14.9	77.7	150.0	-
U-12s	-	-	-	-	-	-
UE-16f	-	-	-	-	-	-
TW-1	-	-	20.0	-	20.0	9.1
UE-17a-831'	-	0.4	829.0	62.5	180.0	-
UE-17a-992'	-	0.8	855.0	44.8	180.0	-
UE-17a-1085'	-	-	314.0	10.7	-	-
UE-18r	80.0	3.5	80.0	-	-	21.6
UE-19h	90.0	7.7	270.0	60.0	20.0	25.5
UE-20bh-1	-	1.0	0.9	4.0	60.0	-
Water Supply Wells						
UE-5c	15.0	4.6	51.1	0.9	70.0	30.9
WW-5c	3.0	6.5	19.4	0.4	-	24.0
WW-C	302.0	6.4	793.0	-	520.0	13.7
WW-C1	299.0	6.4	811.0	0.7	520.0	14.2
WW-4	21.0	5.4	146.0	-	100.0	27.4
UE-16d	-	1.6	434.0	2.7	-	-
WW-8	-	0.6	8.2	1.6	-	-
UE-19c	-	-	-	-	-	19.7
Army Well #1	51.0	2.2	744.0	-	330.0	9.7
J-13	90.0	0.4	36.5	1.2	100.0	27.3
J-12	46.0	0.6	42.0	-	80.0	26.6
GCP Wells						
UE-1-q	10.0	2.3	140.0	-	-	23.8
ER-6-1	30.0	3.3	180.0	-	-	15.8
Post-Shot Wells						
UE-2ce	-	-	-	-	-	-
UE-3e#4-1630'	-	-	-	-	-	-
UE-3e#4-1785'	-	-	-	-	-	-
UE-3e#4-1885'	-	-	-	-	-	-
UE-3e#4-2150'	-	-	-	-	-	-
U-4t-PS-3A	-	-	-	-	-	-
U-4u-PS-2A	-	-	-	-	-	-
UE-7-ns	-	-	-	-	-	-

Table 2: HRMP-FY 92-93

WELL	Cl (mg/L)	SO_4 (mg/L)	HCO_3 (mg/L)	I (µg/L)
UE-1a	26.3	-	*357	-
UE-1b	5.9	-	*184	-
UE-1c-1350	5.6	-	*180	-
UE-1c-1636	5.5	-	*190	-
UE-1h-1979	43.2	-	260	8.0
UE-1h-2137	43.6	2.5	260	5.6
U-3mi-1600	-	-	-	-
U-3mi-1650	-	-	-	-
TW-D	-	-	*225	8.0
UE-5n	14.6	27.2	160	6.8
PW-1	12.0	34.3	100	2.3
PW-2	15.2	26.6	100	4.2
PW-3	10.1	28.9	90	3.4
TW-B	22.6	21.0	100	13.0
U-12s	14.0	-	-	-
UE-16f	18.8	-	*900	3.0
TW-1	3.2	-	*104	2.0
UE-17a-831'	27.7	95.5	200	15.0
UE-17a-992'	28.0	96.0	200	26.0
UE-17a-1085'	43.1	45.0	540	280.0
UE-18r	6.3	-	*164	-
UE-19h	8.5	-	*147	-
UE-20bh-1	-	-	60	2.0
Water Supply Wells				
UE-5c	14.1	45.0	150	3.9
WW-5c	12.3	29.6	270	6.6
WW-C	43.5	65.1	485	6.4
WW-C1	43.6	67.1	480	5.2
WW-4	15.2	42.3	*134	3.1
UE-16d	14.3	59.4	200	12.0
WW-8	9.2	14.2	30	4.0
UE-19c	3.1	-	*37	-
Army Well #1	24.0	54.7	400	3.2
J-13	7.6	17.6	105	3.2
J-12	8.0	21.4	100	3.8
GCP Wells				
UE-1-q	5.3	-	160	-
ER-6-1	9.9	-	210	-
Post-Shot Wells				
UE-2ce	-	-	201	-
UE-3e#4-1630'	240.0	-	>700	-
UE-3e#4-1785'	160.0	-	-	-
UE-3e#4-1885'	-	-	-	-
UE-3e#4-2150'	60.0	-	195	-
U-4t-PS-3A	-	-	<120	-
U-4u-PS-2A	-	-	214	-
UE-7-ns	-	-	104	-

* Bicarbonate calculated from laboratory extractions of total inorganic carbon.

Table 2: HRMP-FY 92-93

WELL	$\delta^{18}O$	δD	$^{14}C_{fmc}$	$\delta^{13}C$	^{14}C age
UE-1a	-	-	0.605	-8.6	4,209
UE-1b	-	-	0.160	-4.5	14,996
UE-1c-1350	-	-	0.026	-4.6	28,987
UE-1c-1636	-	-	0.026	-5.3	28,987
UE-1h-1979	-	-	-	-	-
UE-1h-2137	-	-	-	-	-
U-3mi-1600	-	-	-	-	-
U-3mi-1650	-	-	-	-	-
TW-D	-	-	-	-	-
UE-5n	-	-	-	-	-
PW-1	-	-	0.167	-7.3	14,790
PW-2	-	-	0.338	-	8,979
PW-3	-	-	0.210	-7.4	12,897
TW-B	-	-	-	-	-
U-12s	-	-	-	-	-
UE-16f	-	-	-	-	-
TW-1	-	-	0.301	-10.2	9,925
UE-17a-831'	-	-	-	-	-
UE-17a-992'	-	-	-	-	-
UE-17a-1085'	-	-	-	-	-
UE-18r	-	-	0.082	-1.4	20,281
UE-19h	-	-	0.094	-3.3	19,546
UE-20bh-1	-	-	-	-	-
Water Supply Wells					
UE-5c	-	-	-	-	-
WW-5c	-	-	-	-	-
WW-C	-	-	-	-	-
WW-C1	-	-	0.010	-	37,827
WW-4	-	-	-	-	-
UE-16d	-	-	-	-	-
WW-8	-	-	-	-	-
UE-19c	-	-	0.114	-5.3	17,737
Army Well #1	-	-	0.054	-	24,129
J-13	-	-	-	-	-
J-12	-	-	-	-	-
GCP Wells					
UE-1-q	-	-	0.077	-2.4	20,650
ER-6-1	-	-	0.021	-0.7	31,900
Post-Shot Wells					
UE-2ce	-	-	-	-	-
UE-3e#4-1630'	-	-	-	-	-
UE-3e#4-1785'	-	-	-	-	-
UE-3e#4-1885'	-	-	-	-	-
UE-3e#4-2150'	-	-	-	-	-
U-4t-PS-3A	-	-	-	-	-
U-4u-PS-2A	-	-	-	-	-
UE-7-ns	-	-	-	-	-

Table 2: HRMP-FY 92-93

WELL	$^{36}Cl/Cl \times 10^{-13}$	^{36}Cl atoms $\times 10^{7}$	$^{87}Sr/^{86}Sr$	$^{234}U/^{238}U$
UE-1a	8.63	38.6	0.70959	-
UE-1b	6.26	6.3	0.70953	-
UE-1c-1350	7.14	6.8	-	-
UE-1c-1636	7.22	6.7	-	-
UE-1h-1979	1.52	11.2	-	-
UE-1h-2137	1.71	12.7	-	-
U-3mi-1600	-	-	-	-
U-3mi-1650	-	-	-	-
TW-D	7.24	-	-	-
UE-5n	423.00	1049.3	0.70931	-
PW-1	8.42	17.2	-	-
PW-2	5.27	13.6	0.71116	-
PW-3	6.78	11.6	-	-
TW-B	9.42	36.2	-	-
U-12s	3.35	8.0	-	-
UE-16f	3.12	10.0	-	-
TW-1	9.68	5.3	0.70893	-
UE-17a-831'	5.85	27.5	-	-
UE-17a-992'	5.66	26.9	-	-
UE-17a-1085'	3.58	26.2	-	-
UE-18r	6.36	6.8	0.70909	-
UE-19h	4.79	6.9	-	-
UE-20bh-1	6.45	-	-	-
Water Supply Wells	-	-	-	-
UE-5c	6.13	14.7	0.70975	-
WW-5c	6.96	14.5	0.71074	-
WW-C	1.76	13.0	0.71503	-
WW-C1	1.66	12.3	0.71506	-
WW-4	6.16	15.9	-	-
UE-16d	6.36	15.5	-	-
WW-8	5.83	9.1	-	-
UE-19c	6.26	3.3	0.70943	-
Army Well #1	4.28	17.5	0.71196	-
J-13	5.02	6.5	0.71155	-
J-12	5.03	6.8	0.71162	-
GCP Wells				
UE-1-q	7.90	7.10	0.71129	0.000268
ER-6-1	3.92	6.59	0.71283	0.000229
Post-Shot Wells				
UE-2ce	-	-	-	-
UE-3e#4-1630'	-	-	-	-
UE-3e#4-1785'	-	-	-	-
UE-3e#4-1885'	-	-	-	-
UE-3e#4-2150'	-	-	-	-
U-4t-PS-3A	-	-	-	-
U-4u-PS-2A	-	-	-	-
UE-7-ns	-	-	-	-

Table 2: HRMP-FY 92-93

WELL	$^{4}He \times 10^{12}$ atm/ml	$^{129}Xe \times 10^{10}$	$^{82}Kr \times 10^{11}$	$^{20}Ne \times 10^{12}$	$^{36}Ar \times 10^{13}$
UE-1a	-	-	-	-	-
UE-1b	-	-	-	-	-
UE-1c-1350	-	-	-	-	-
UE-1c-1636	-	-	-	-	-
UE-1h-1979	-	-	-	-	-
UE-1h-2137	-	-	-	-	-
U-3mi-1600	-	-	-	-	-
U-3mi-1650	-	-	-	-	-
TW-D	-	-	-	-	-
UE-5n	-	-	-	-	-
PW-1	-	-	-	-	-
PW-2	-	-	-	-	-
PW-3	-	-	-	-	-
TW-B	-	-	-	-	-
U-12s	-	-	-	-	-
UE-16f	-	-	-	-	-
TW-1	-	-	-	-	-
UE-17a-831'	-	-	-	-	-
UE-17a-992'	-	-	-	-	-
UE-17a-1085'	-	-	-	-	-
UE-18r	-	-	-	-	-
UE-19h	-	-	-	-	-
UE-20bh-1	-	-	-	-	-
Water Supply Wells	-	-	-	-	-
UE-5c	-	-	-	-	-
WW-5c	-	-	-	-	-
WW-C	-	-	-	-	-
WW-C1	-	-	-	-	-
WW-4	-	-	-	-	-
UE-16d	-	-	-	-	-
WW-8	-	-	-	-	-
UE-19c	-	-	-	-	-
Army Well #1	-	-	-	-	-
J-13	-	-	-	-	-
J-12	-	-	-	-	-
GCP Wells					
UE-1-q	1.76	5.81	1.92	4.27	2.51
ER-6-1	10.10	6.01	2.09	7.14	2.96
Post-Shot Wells					
UE-2ce	-	-	-	-	-
UE-3e#4-1630'	-	-	-	-	-
UE-3e#4-1785'	-	-	-	-	-
UE-3e#4-1885'	-	-	-	-	-
UE-3e#4-2150'	-	-	-	-	-
U-4t-PS-3A	-	-	-	-	-
U-4u-PS-2A	-	-	-	-	-
UE-7-ns	-	-	-	-	-

Table 2: HRMP-FY 92-93

WELL	^{3}H (TU)	^{85}Kr (pCi/L)	^{90}Sr (pCi/L)	^{99}Tc (pCi/L)	^{60}Co (pCi/L)
UE-1a	-	-	-	<5	<0.680
UE-1b	-	-	-	<5	<0.437
UE-1c-1350	-	-	-	<5	<0.472
UE-1c-1636	-	-	-	<5	<0.582
UE-1h-1979	3.4±0.6	-	-	<5	-
UE-1h-2137	1.9±0.5	-	-	<5	-
U-3mi-1600	-	-	-	<5	-
U-3mi-1650	-	-	-	<5	-
TW-D	1.2±0.4	-	-	<5	-
UE-5n	3079±161	-	-	<5	-
PW-1	0.1±0.2	-	-	<5	-
PW-2	0.2±0.2	-	-	<5	-
PW-3	1.2±0.3	-	-	<5	-
TW-B	-	-	-	<5	<0.667
U-12s	-	-	-	<5	-
UE-16f	-	-	-	<5	-
TW-1	-	-	-	<5	-
UE-17a-831'	-	-	-	<5	-
UE-17a-992'	0.0±0.2	-	-	<5	-
UE-17a-1085'	0.5±0.2	-	-	<5	-
UE-18r	-	-	-	<5	<0.631
UE-19h	-	-	-	<5	<0.455
UE-20bh-1	0.3±0.2	-	-	<5	-
Water Supply Wells	-	-	-		-
UE-5c	0.2±0.2	-	-	<5	-
WW-5c	0.2±0.2	-	-	<5	-
WW-C	3.6±0.5	-	-	<5	-
WW-C1	-	-	-	-	-
WW-4	0.3±0.2	-	-	<5	-
UE-16d	19.8±12.0	-	-	<5	-
WW-8	0.5±0.3	-	-	<5	-
UE-19c	0.5±0.2	-	-	<5	<0.699
Army Well #1	0.4±0.2	-	-	<5	-
J-13	0.2±0.2	-	-	<5	-
J-12	0.2±0.2	-	-	<5	-
GCP Wells					
UE-1-q	<0.3	<30	<0.9	<5	<0.590
ER-6-1	<0.3	<30	<0.9	<5	<0.400
Post-Shot Wells	**field scans**				
UE-2ce	40,625	-	-	-	-
UE-3e#4-1630'	137,500	-	-	-	-
UE-3e#4-1785'	15,000	-	-	-	-
UE-3e#4-1885'	10,313	-	-	-	-
UE-3e#4-2150'	2,937,500	-	-	-	-
U-4t-PS-3A	12,188	-	-	-	-
U-4u-PS-2A	15,000,000	-	-	-	-
UE-7-ns	144	-	-	-	-

Table 2: HRMP-FY 92-93

WELL	^{125}Sb (pCi/L)	^{137}Cs (pCi/L)
UE-1a	<1.90	<0.695
UE-1b	<1.32	<0.427
UE-1c-1350	<1.43	<0.455
UE-1c-1636	<1.65	<0.583
UE-1h-1979	-	-
UE-1h-2137	-	-
U-3mi-1600	-	-
U-3mi-1650	-	-
TW-D	-	-
UE-5n	-	-
PW-1	-	-
PW-2	-	-
PW-3	-	-
TW-B	<1.90	<0.706
U-12s	-	-
UE-16f	-	-
TW-1	-	-
UE-17a-831'	-	-
UE-17a-992'	-	-
UE-17a-1085'	-	-
UE-18r	<1.82	<0.609
UE-19h	<1.36	<0.437
UE-20bh-1	-	-
Water Supply Wells	-	-
UE-5c	-	-
WW-5c	-	-
WW-C	-	-
WW-C1	-	-
WW-4	-	-
UE-16d	-	-
WW-8	-	-
UE-19c	<1.93	<0.641
Army Well #1	-	-
J-13	-	-
J-12	-	-
GCP Wells		
UE-1-q	<1.80	<0.650
ER-6-1	<1.20	<0.400
Post-Shot Wells	-	-
UE-2ce	-	-
UE-3e#4-1630'	-	-
UE-3e#4-1785'	-	-
UE-3e#4-1885'	-	-
UE-3e#4-2150'	-	-
U-4t-PS-3A	-	-
U-4u-PS-2A	-	-
UE-7-ns	-	-

APPENDIX 1: Sampling Procedures For Isotopic Analyses of Groundwater

Noble Gases (for pumped wells only)

Sampling containers: Copper tube mounted between two pinch clamps on a metal base; three to four per well.

1. Label the copper tube with a Sharpie pen.
2. Attach the small diameter hose to the large diameter hose, then to the copper tube. Attach the extra length of plain tygon tubing to the outlet end of the copper tubing.
3. One person must hold the outlet end of the plain tygon tubing above the level of the copper tubing. This prevents any modern atmosphere from entering the sample.
4. Obtain a slow, non-turbulent water flow using the regulator and/or splitter.
5. Dislodge any air bubbles by lightly striking the hose and copper tubing with the ratchet wrench.
6. Use the wrench to tighten the pinch clamps. Pinch the outlet end of the copper tube first. Be very careful that the small diameter hose at the inlet end of the copper tube does not blow-off from the increase in pressure. It may be necessary to stop the flow of water with the regulator once the outlet end of the copper tube has been completely pinched off. Care must be taken not to over flex the pinch in the copper tube as this will destroy the air tightness of the copper tube and compromise the sample.
7. Tighten the pinch clamps at the inlet end of the copper tube. Remove all tygon tubing from the copper tubing.

NOTE: Collect a minimum of three samples per well; preferably four samples.

^{18}O & D/H (steps 1 and 2 for pumped wells only).

Sampling containers: two 30 ml glass bottles.

1. Rinse the outside before opening the bottle to remove any accumulation of dust on the bottle surface.

2. Fill the bottle with approximately 15 mls of water, cap and shake. Discard this bottle rinse.
3. Fill the bottle leaving about 3 mls (or 10% of the bottle volume) of headspace. Make sure the cap is sealed properly so as not to promote evaporation and compromise the sample.
4. Dry and label the bottle.
5. Single bag the bottle and tape the bag closed.

^{3}H (steps 1 and 2 for pumped wells only).

Sample container: one 0.5 liter glass bottle.

1. Rinse the outside before opening the bottle to remove any accumulation of dust on the bottle surface.
2. Fill the bottle with approximately 250 mls of water, cap and shake. Discard this bottle rinse.
3. Fill the bottle completely leaving a small headspace.
4. Single bag the bottle and tape the bag closed.

^{36}Cl (steps 1 and 2 for pumped wells only).

Sampling container: 1-liter plastic I-Chem bottle

1. Rinse the outside before opening the bottle to remove any accumulation of dust on the bottle surface.
2. Fill the bottle with approximately 2 liters of water, cap and shake. Discard this bottle rinse.
3. Fill the bottle to the black mark on the shoulder of the bottle.
4. Dry and label the bottle.
5. Single bag the bottle and tape the bag closed.

^{14}C (steps 2-4 for pumped wells only).

Sampling container: 1-liter glass bottle (cleaned & acid leached)

1. Latex gloves must be worn when touching the bottle, and the first bag that covers the bottle, and during the addition of $HgCl_2$.
2. Rinse the outside of the bag before opening to remove any accumulation of dust on the bag surface.
3. Fill the bottle with approximately 500 mls of water, cap and shake. Discard this bottle rinse.
4. Insert the short tygon tubing, attached beneath the I-Chem bottle cap, into the bottle and fill. NOTE: The tygon tubing inserted into the bottle is not to touch anything else except the plastic I-Chem bottle with which it is stored. Allow at least one bottle volume to overflow. Leave about 5 ml headspace.
5. Dry, label and single bag the bottle. Tape the bag closed to keep dust off the bottle.
6. In a sheltered area (the trailer in Mercury), add 4 drops saturated aqueous mercuric chloride solution using a cleaned disposable pipette.

NOTE: Keep the saturated aqueous mercuric chloride away from any acids.

7. Double bag the bottle with two *new* clean bags. Tape the bags closed.

$^{234}U/^{238}U$ & $^{87}Sr/^{86}Sr$ (steps 2 and 6 for pumped wells only).

Sampling container: One acid leached 1-liter plastic I-Chem bottle.

1. Attach 0.45mm filter to the appropriate hoses such that the flow arrow on the filter capsule points up.
2. Purge 5-8 minutes while keeping the flow arrow on the filter pointing up.
3. Latex gloves must be worn when touching the bottle or the first bag that covers the bottle.
4. Rinse the outside of the bag before opening to remove any accumulation of dust on the bag surface.

5. Rinse the outside of the bottle before opening to remove any accumulation of dust on the bottle surface.
6. Fill the bottle with approximately 500 mls of water, cap and shake. Discard this bottle rinse.
7. Insert the short tygon tubing, attached beneath the I-Chem bottle cap, into the bottle and fill. NOTE: The tygon tubing inserted into the bottle is not to touch anything else except the plastic I-Chem bottle with which it is stored. Allow at least one bottle volume to overflow (not for bailed wells). Leave about 5 ml headspace.
8. Dry, label and single bag the bottle. Tape the bag closed to keep dust off the bottle.
9. In a sheltered area (trailer in Mercury), add HNO_3 to each bottle to achieve a pH of 2.
10. Secure the cap with a strip of parafilm. (i.e. wrap parafilm around the cap to prevent leakage during shipping).
11. Tape the bag.
12. Add a second bag and tape it.

^{90}Sr (steps 2 and 4-6 for pumped wells only).

Sampling container: 1-liter plastic I-Chem bottle.

1. Attach 0.45mm filter to the appropriate hoses such that the flow arrow on the filter capsule points up.
2. Purge 5-8 minutes while keeping the flow arrow on the filter pointing up.
3. Laytex gloves must be worn when touching the bottle or the first bag that covers the bottle.
4. Rinse the outside of the bag before opening to remove any accumulation of dust on the bag surface.
5. Rinse the outside of the bottle before opening to remove any accumulation of dust on the bottle surface.

6. Fill the bottle with approximately 500 mls of water, cap and shake. Discard this bottle rinse.
7. Insert the short tygon tubing, attached beneath the I-Chem bottle cap, into the bottle and fill. NOTE: The tygon tubing inserted into the bottle is not to touch anything else except the plastic I-Chem bottle with which it is stored. Allow at least one bottle volume to overflow. Leave about 5 ml headspace.
8. Dry, label and single bag the bottle. Tape the bag closed to keep dust off the bottle.
9. In a sheltered area (trailer in Mercury), add HNO_3 to each bottle to achieve a pH of 2.
10. Secure the cap with a strip of parafilm. (i.e. wrap parafilm around the cap to prevent leakage during shipping).
11. Tape the bag.
12. Add a second bag and tape it.

^{99}Tc (steps 1 and 2 for pumped wells only).

Sampling container: 4-liter plastic I-Chem bottle

1. Rinse the outside before opening the bottle to remove any accumulation of dust on the bottle surface.
2. Fill the bottle with approximately 2 liters of water, cap and shake. Discard this bottle rinse.
3. Fill the bottle to the black mark on the shoulder of the bottle.
4. Dry and label the bottle.
5. Single bag the bottle and tape the bag closed.

^{137}Cs, ^{60}Co & ^{125}Sb (steps 1 and 2 for pumped wells only).

Sample container: one 1-liter plastic I-Chem bottle.

1. Rinse the outside before opening the bottle to remove any accumulation of dust on the bottle surface.

2. Fill the bottle with approximately 500 mls of water, cap and shake. Discard this bottle rinse.
3. Fill the bottle to the shoulder.
4. Single bag the bottle and tape the bag closed.

^{85}Kr (for pumped wells only).

Sampling container: one 1-liter stainless steel evacuated cylinder.

1. Remove and save the closed-end nuts, used for shipping, from both ends of the cylinder.
2. Place the free end of the small diameter tygon tubing over one end of the now-bear threads.
3. While holding the cylinder vertical, with the hose end pointing down, slowly open the bottom knob, closest to the attached hose. A hissing sound associated with the filling of the cylinder can be heard.
4. Allow the cylinder to fill.
5. When the cylinder is full (often the temperature of the water is sufficiently different from that of the stainless steel cylinder that the water level in the cylinder can be easily determined), slowly open the top knob while keeping the cylinder vertical.
6. Allow 2-3 cylinder volumes (2-3 liters) to overflow.
7. Close the top knob first, then quickly close the bottom knob.

NOTE: Because of the pressure build-up associated with several steps in this procedure, all steps must be carried out quickly. The pressure of the water may be adjusted before beginning sampling.

For bailed wells, collect a sealed bailer for shipment back to LLNL.

APPENDIX 2: Analytical Techniques

All analyses were completed at the Nuclear Chemistry Division of Lawrence Livermore Lab unless otherwise stated. Analyses for field ^{3}H were completed using standard scintillation counting techniques at the NTS.

The Tc for ^{99}Tc determination was separated and concentrated by resins and analyzed by liquid scintillation counting (Silva et al., 1986). One liter of the sample was oxidized with HCl and H_2O_2 and mixed with 0.5 grams of AG 1 x 8 (100-200 mesh) anion resin. After 4 hours of stirring, the resin was separated and stacked in a column, and then converted from the chloride form to the perchlorate form with 2cc of $NaClO_4$. The Tc was reduced and eluted from the column with a 1M $NaClO_4$-0.02M Na_2SO_3 solution. Two milliliters of the sample was mixed with 15cc of scintillation cocktail and counted.

In the Sr purification for ^{90}Sr analysis, the water sample was mixed with a 2mg Sr carrier, evaporated down to a dry residue in a teflon beaker and then redissolved with 2cc of 6N HNO_3. The dissolved sample was loaded onto a Sr-Spec resin column and washed 6 times with 6N HNO_3 (Horwitz et al., 1990). The Sr was removed from the resin with 0.05N HNO_3, mixed with a 20mg yittrium carrier, and equilibrated for 28 days allowing ^{90}Y to grow. The Y was then separated from the Sr by the same resin technique as above. A saturated solution of $(NH_4)_2C_2O_4$ was added to the Y extract. The mixture was then filtered and the residue ashed into a yittrium oxide. The oxide was sandwiched between mylar and beta counted.

The ^{60}Co, ^{125}Sb, ^{137}Cs activities were counted using a cylindrical Marinelli beaker with a well design for a standard up-looker cryostat (Failor et al., 1988). The cryostat contains a high purity germanium gamma-ray detector. Samples were untreated and counted for approximately 1 week. Raw data was reduced using the GAMANAL software (Gunnink and Niday, 1972).

The ^{36}Cl was extracted by precipitating a quantitative yield of Cl from the water by adding $AgNO_3$ and precipitating a AgCl solid (Bentley et al., 1986). The AgCl was then dissolved in NH_4OH to precipitate out any sulfates. The aqueous solution was filtered and AgCl was reprecipitated by acidification. The precipitate was then washed, dried-down, and packed into an aluminum target. The ^{36}Cl was separated from the AgCl by Cs source ionization and accelerator mass spectrometry (Elmore et al., 1979), and the analysis was reported as a ratio of ^{36}Cl to total Cl in the water.

The inorganic carbon was extracted from the sample by vacuum line acid stripping of the water using 5 ml of 100% phosphoric acid to acidify the sample to a pH <1. Carbon dioxide liberation from the sample was further facilitated by an ultrapure nitrogen carrier gas. The CO_2 was cryogenically trapped and separated from the water. The CO_2 was split for ^{13}C analysis by stable isotope mass spectrometry, completed at the University of California, Davis Geology Department. The carbon dioxide for ^{14}C was reduced on a separate vacuum line to graphite using a cobalt catalyst and hydrogen gas at a 570°C reaction temperature, and ^{14}C concentrations were determined by accelerator mass spectrometry.

For $^{87}Sr/^{86}Sr$ ratio determination, the water sample was evaporated down to a dry residue in a teflon beaker and then redissolved with 2cc of 6N HNO_3. The dissolved sample was loaded onto a Sr-Spec resin column and washed 6 times with 6N HNO_3 (Horwitz et al., 1990). The Sr was removed from the resin with 0.05N HNO_3, and the Sr extract was dried-down. The residue was baked onto a tantalum filament and analyzed for its $^{87}Sr/^{86}Sr$ ratio by thermal ionization mass spectrometry.

For $^{234}U/^{238}U$ ratio determination, an aliquot of the water sample was added to a 10mg/ml $FeCl_2$ solution. The mixture was adjusted to pH 8 with NH_4OH and the U was precipitated out with $Fe(OH)_3$ (Goldberg et al., 1963). The precipitate was collected, acidified, and the U was separated with a uranium specific resin. The U extract was

dried-down, baked onto a triple Re filament, and its $^{234}U/^{238}U$ ratio was determined by thermal ionization mass spectrometry.

The Kr for ^{85}Kr analysis was separated by gas chromatography. Thirty cm^3 STP Kr carrier were added to the sample. The water was frozen to -77°C and the remaining gas was collected onto activated charcoal at -196°C. The O_2, N_2, and Ar were separated from the Kr by a He elution at -36°C. The Kr was transferred at 23°C to a 5A molecular sieve at -196°C. The temperature was raised to -36°C and the Kr was collected on activated charcoal with yields of about 95% and purities of about 99%. The Kr was loaded into thin window Beta counting cells and counted for 360 minutes with an external detector of 8% efficiency.

For $^3He/^4He$ determination the sample was attached to the noble gas sample manifold with an all metal helium-tight seal and the section was evacuated. The water sample was released by removing a clamp and re-rounding the pinched copper tube. The water was collected in a 200 cm^3 volume. The water was frozen with liquid nitrogen after 10 min, where the majority of the He (>99%) was left in the gas phase. Active gases were removed with a hot Ti-Al alloy (400°C) getter. Argon, krypton and xenon were collected on activated charcoal at liquid nitrogen temperature. Helium and neon were collected on activated charcoal at -263°C. The helium was then released into the mass spectrometer at -238°C. The mass spectrometer was operated at a resolving power of about 600 and the HD peak was completely resolved from the ^3He peak. The mass 3 detector was a 17 stage dynode electron multiplier. The mass 4 detector was a faraday cup. The relative sensitivity of the two detectors was calibrated by analyzing samples of air helium with $^3He/^4He=1.40 \times 10^{-6}$.

For determination of the He, Ne, Ar, Kr and Xe abundances the water sample was released into a 200 cm^3 volume as described in step 1 above except that just prior to release, standard quantities of ^3He, ^{21}Ne, ^{38}Ar, ^{80}Kr and ^{124}Xe were added to the volume from a gas aliquotting system (2 liter reservoir volume plus a 0.2 cm^3 aliquotting

volume). The water sample was frozen with liquid nitrogen and then thawed and warmed to 50°C. The sample was then frozen again with dry ice (-78°C). This process was to mix the sample gases with the spike gases (^{3}He, ^{21}Ne, ^{38}Ar, ^{80}Kr and ^{124}Xe). A small aliquot of the gas (1%) was taken for argon analysis. The gas was purified by exposure to hot Ti-Al alloy getters and then the gas was admitted to the mass spectrometer for isotopic analysis. The remaining gas was purified by gettering, and then the Ar, Kr and Xe were collected on activated charcoal. The He and Ne were split into two samples. First the He was analyzed, then the Ne was analyzed. The charcoal trap containing the Kr and Xe was warmed slightly to desorb the Ar, and the Ar was pumped away. The Kr and Xe were then completely released and admitted to the mass spectrometer. The Kr and Xe were measured simultaneously. The measurements were calibrated by using samples of water prepared in the laboratory (mostly at 21°C, 600' elevation). Analytical uncertainty is approximately 2%.

DATE

FILMED

6/30/94

END